

THE PRESENT STATUS OF QUANTUM ELECTRODYNAMICS⁺

Stanley J. Brodsky^{*}

and

Sidney D. Drell

Stanford Linear Accelerator Center, Stanford University
Stanford, California 94305

(Submitted to Annual Review of Nuclear Science)

⁺Work supported in part by the U.S. Atomic Energy Commission.

^{*}Temporary address until August 1970: Laboratory of Nuclear Studies, Cornell University, Ithaca, New York 14850.

1. INTRODUCTION¹

Origins of the theory.--Quantum electrodynamics (QED) is the theory of interacting photons, electrons, and muons. In a more complete description we also include their electromagnetic interactions with hadrons as well as their couplings with weak currents, all of which contribute if we probe with sufficient precision.

QED is a great theory--it works! Since recent experimental and theoretical progress has not only dispersed all clouds casting any shadows of doubt as to its successes from the terrain of its applications but has also extended its realm of triumphs, this is an opportune time to review and praise QED.

QED has a very simple conceptual basis and indeed is built by purely imitative steps. Shortly after the birth of quantum mechanics it was constructed very simply by applying the ordinary rules of the quantum theory to the electromagnetic field amplitudes, $E(y,t)$ and $B(y,t)$, whose space-time development is given by the Maxwell equations. Thus, as had originally happened to the position and momentum coordinates of a single particle, the field amplitudes also became operators whose matrix elements are observable.

This quantum transcription proceeded by the following steps: For a single particle the canonical position and momentum variables x and p are replaced as observables by transition matrix elements $\langle f|x|i\rangle$ and $\langle f|p|i\rangle$ where $|i\rangle$ and $\langle f|$ customarily denote energy eigenstates. Their energy difference is proportional to the frequency of light emitted or absorbed in transitions between them as a result of their interaction with radiation:

$E_f - E_i = h\nu$. For a physical system composed of several or more particles we have corresponding canonical coordinates (x_k, p_k) , $k = 1, \dots, N$ for each of the N degrees of freedom, and apply the quantum transcription to each coordinate.

As the number N becomes very large it is often more convenient to describe a system in the continuum language rather than in terms of a discrete sum over $N \rightarrow \infty$. Thus we describe a vibrating string not in terms of the displacements of each atom as a function of time, $x_k(t)$, but rather in terms of a continuous displacement "field" $x(y,t)$ which records the time development as a function of the position along the length of the string $0 \leq y \leq L$. The continuous variable y replaces the discrete index k and a net of N coupled total differential equations is replaced when $N \rightarrow \infty$ by a single partial differential equation to describe the motion at each point of space and time. Similarly the quantization prescription can be applied in its continuum limit to the "field" $x(y,t)$.

We treat the electromagnetic fields $E(y,t)$ and $B(y,t)$ analogously. At each point of space time (y,t) they themselves are generalized coordinates to be given the same quantum mechanical transcription as $x(y,t)$, the continuum limit of $x_k(t)$. This is the canonical quantization procedure first developed by Heisenberg and Pauli in 1929 and from this treatment there emerge photons as quanta of the Maxwell fields (1).

An analogous language must be invented to describe the electron-positron field. In going from a classical to a quantum dynamical description as described earlier, notions such as

energy eigenstates, wave functions, and probability are born. These provide a nonrelativistic framework for describing the motion of a single particle, for example, in terms of a wave function $\psi(y,t)$ satisfying the Schrodinger equation. However, when we expand this framework to meet the requirements of the theory of special relativity--which are automatically met by the Maxwell equations describing light and photons--we can no longer speak in general of one electron. We must now speak of positrons as well as electrons.

With the appearance of anti-matter which necessarily accompanies the negative energy root in the quadratic Einstein energy-momentum relation $E^2 = p^2 c^2 + m_0^2 c^4$, and with the possibility of electromagnetic waves converting to electron-positron pairs, and vice versa, we no longer have a one particle quantum mechanics with the simple probability interpretation of Heisenberg and Schrodinger. The formalism for creating and destroying these pairs is constructed largely in parallel with that introduced to quantize Maxwell. The wave function of an electron introduced in the Schrodinger theory now becomes an operator which creates and destroys single electrons and positrons just as $E(y,t)$ and $B(y,t)$ did for photons. This second application of the quantum principle to the electron coordinate--or "second quantization"--gives finally the Dirac theory for the interaction of radiation and electron fields in accord with the principles of special relativity and quantum theory. From a conceptual point of view we have taken no revolutionary steps.

Implications of locality.--Before continuing on and exploring the experimental consequences of this approach of applying the

quantization procedure to classical fields which satisfy wave equations, let us discuss briefly some of the implications of such a program. First of all we end up with a theory with differential wave propagation. Both the notions of local fields and of point interactions are taken over from the classical theory. The field amplitudes are continuous functions of parameters y and t and the changes in the fields at a point y are determined by properties of the fields infinitesimally close to the point y .

We may wonder whether this prescription is only an idealization that can be adopted in the sense of a correspondence principle. It may be a sufficiently precise description when the theory is being tested by low-resolution probes that "see" the average behavior of the system over a volume of dimensions of the order of the electron Compton wavelength, $\hbar/m_e c \approx 3.9 \times 10^{-11}$ cm. However, if we look with a higher resolution microscope at dimensions comparable to, say, the nucleon Compton wavelength, $\hbar/Mc \approx 2 \times 10^{-14}$ cm, an elementary space-time structure or granularity may reveal itself. This is in fact what occurs for most physical systems. Sound waves or vibrating membranes, for example, are described by wave fields. However, such a wave description is an idealization valid only for distances larger than a characteristic length that measures the structure of the medium (the interatomic separation $\sim 1 \text{ \AA}$ or 10^{-8} cm). At smaller distances there are indeed profound modifications in these theories. The Debye theory of specific heat of a crystal lattice is a familiar example of major corrections to a continuum description for excitations on an atomic scale.

On the scale of atomic dimensions no comparable granularity is

observed for the electromagnetic field. In fact, it was just the absence of any evidence for the existence of an "ether" or of any need for a mechanistic interpretation of the radiation field that led to Einstein's theory of special relativity. Now we take it for granted that both photon and electron fields satisfy differential wave equations and exhibit local interactions. We should recognize, however, the enormity of the extrapolation of this concept from atomic ($\sim 10^{-8}$ cm) to electron ($\sim 10^{-11}$ cm) and eventually to nuclear ($\sim 10^{-14}$ cm) dimensions, and we must ask whether this description may falter ever so slightly along the way.

Have we any suspicions of troubles on the way down to the nuclear domain of 10^{-14} cm? From a purely theoretical viewpoint we recall from classical electromagnetic theory that the self energy of a charge distribution of radius a_0 and total charge e is $\sim e^2/a_0$ which is the work necessary to assemble such a structure. This work increases with decreasing a_0 and becomes infinite for the self energy of a point charge. Since the particles are points in QED and have local interactions we may expect that here too the self energies will be infinitely large--a discomfoting if not puzzling result if true. Indeed in weak coupling perturbation calculations the divergence of the self energy remains, even though softened from a linear to logarithmic behavior, i.e., $\frac{1}{a_0} \rightarrow \ln a_0$. It was the great achievement of Feynman, Schwinger, and Tomonaga (1) above all that a renormalization theory was formulated that allowed the theory to coexist peacefully with such divergences and yield finite unambiguous answers for experimentally observable quantities. However it is a fact that, at least in perturbation

theory, the renormalization constants are infinite so that each calculation of a physical quantity has an infinity buried in it. Whether this infinity is a disease of the mathematical techniques of perturbation expansions, or whether it is symptomatic of the ills accompanying the idealization of a continuum theory we don't know. Perhaps there is a "fundamental length" at small distances that regularize these divergences.

The only way to find out is to probe with experiments at ever smaller dimensions. Theory can never provide the answer to questions like this. In principle the data are required--and also in practice, since theory has not succeeded in developing a workable formalism freed from the confining bonds of a point interaction. So we must probe experimentally for evidence of a breakdown in our notions of local fields and action, and we must look to the data for evidence of the ultimate granularity, or fundamental length.

Mirabile dictu, as of the present, there is no evidence that QED fails to meet the challenge. Including the classical domain of Maxwell's equations which quantitatively reproduce the pattern of the earth's magnetic field as observed near the surface of the earth and from satellites in space, QED has been applied with complete and fantastic success over a range of 24 decades from the subnuclear realm of 10^{-14} cm out to a limit of 5.5×10^{10} cm (about 80 earth radii) for the Compton wavelength of the photon (2).

2. HIGH MOMENTUM TESTS OF QED

How to accomplish high momentum transfers.--How can we find out what is going on in this region? One way is to take the high-energy-road of experiments with very large momentum transfers q that probe distances R of the order of $R \sim \hbar/q \sim 10^{-14}$ cm for $q \sim 2$ GeV/c to an accuracy of several percent. Such high momentum transfers can best be realized in colliding beam experiments, e.g. electron-electron or electron-positron scattering. Colliding beams are necessary because otherwise very energetic incident electrons appear as massive projectiles in the relativistic sense striking light target electrons. In such a case, a multi-GeV electron beam incident on a target electron (essentially at rest in its atomic orbit) loses most of its effective energy by having to conserve center of mass motion, and momentum transfers only up to 150 MeV/c are realizable at present.

If we denote the incident electron energy in the laboratory reference system by E_0 and its rest energy by $m_0 c^2$, then the invariant four-momentum transfer in a scattering through laboratory angle θ is

$$\Delta q = (-q_\mu q^\mu)^{1/2} = \frac{2E_0/c \sin \frac{\theta}{2}}{\left[1 + 2E_0/m_0 c^2 \sin^2 \frac{\theta}{2}\right]^{1/2}} < (2m_0 E_0)^{1/2}, \quad 2.1$$

and increases only as $E_0^{1/2}$. This means that for incident electron energies up to $E_0 \sim 40$ BeV, a maximum realizable energy for the foreseeable future, $q < 200$ MeV/c, corresponding to a length $\lambda_{\Delta q} = \hbar/\Delta q > 10^{-13}$ cm.

To avoid this one can also do experiments such as wide-angle

electron (or muon) pair photoproduction in which the target proton is used to anchor the center of mass. The unknown proton structure form factors can be factored out by comparison between these and elastic scattering processes. ~~#~~ The alternate route is along the low-energy road of very high precision atomic and resonance experiments (in particular, very precise measurements of the Lamb shift and hyperfine structure) and the free electron (or muon) gyromagnetic ratio. This will be discussed in the next section. On the high-energy-road the normalization and statistical errors in the experiments are typically 5 - 7%, and thus we need only discuss the lowest order, or Born amplitudes. Generally the radiative and higher order Born corrections are smaller. In any case, they have been calculated in general and included in the analyses.

Colliding rings.--For electron-electron, or Moller, scattering the two Born diagrams are shown in Fig. 1. The invariant momentum transfers are spacelike in both cases, and are given by

$$\begin{aligned}
 q^2 &= -E_{\text{cm}}^2 \sin^2 \frac{\theta}{2} = t \\
 \text{or} \quad q^2 &= -E_{\text{cm}}^2 \cos^2 \frac{\theta}{2} = u
 \end{aligned}
 \tag{2.2}$$

where $E_{\text{cm}} = \sqrt{s}$ is the total energy of both colliding electrons and θ is the scattering angle in the colliding ring frame.

$q^2 = t$ or u depending on which of the indistinguishable electrons is detected, i.e., depending on whether or not the electron line is exchanged as illustrated.

The pioneering measurements (3) of e^-e^- elastic scattering date back to 1965 on the Princeton-Stanford storage ring at

$\sqrt{s} = 1100$ MeV. In this experiment the angular dependence of the cross section was tested but not the absolute magnitude. The detailed analysis of the radiative corrections in terms of actual experimental resolutions, as developed by Y. S. Tsai, was included in the comparison with theory. As a simple mnemonic for making this comparison it is convenient to assume a modification factor for the photon propagator of the form

$$-\frac{1}{q^2} \rightarrow -\left[\frac{1}{q^2} \pm \frac{1}{q^2 - K^2}\right] \quad 2.3$$

In terms of a space-time picture 2.3 corresponds to a small distance modification of the Coulomb potential to

$$\frac{1}{r} \rightarrow \frac{1}{r} \left[1 \pm e^{-Kr/\hbar}\right]. \quad 2.4$$

The form with the plus sign between the two terms corresponds to adding "heavy photon" terms to the amplitude with which the photon propagates between the vertices in Fig. 1 and satisfies all general conditions of causality, unitarity, and spectrum of usual canonical QED as embodied in the Kallen-Lehmann representation. On the other hand, one need not feel bound to such conditions as he goes in search of a breakdown or fundamental change of QED. Indeed, Lee and Wick (4) have recently shown how to construct a set of working rules with a QED made more convergent at large q^2 by having photons propagate according to 2.3 with the minus sign. The latest experimental results expressed in terms of the modification 2.3 with the minus sign to improve convergence, are (3)

$$K^{-2} = -0.06 \pm 0.06 \text{ (GeV)}^{-2}, \quad \text{(statistical error only)} \quad 2.5$$

which implies with 95% confidence that

$$K > 4 \text{ GeV} \quad \text{or} \quad \hbar/K < 0.5 \times 10^{-14} \text{ cm.} \quad 2.6$$

The corresponding limit on the additive modification is

$$K > 2.4 \text{ GeV} \quad \text{or} \quad \hbar/K < 10^{-14} \text{ cm.} \quad 2.7$$

Elastic electron-positron, or Bhabha, scattering is related to the e^-e^- or Moller scattering by "crossing" the momentum transfer (t and u) channels with the energy (s) channel. This takes Fig. 1 to the Feynman diagrams of Fig. 2, with the corresponding momentum transfers carried by the photon line now given by

$$q^2 = E_{\text{cm}}^2 = s \quad 2.8$$

and
$$q^2 = -E_{\text{cm}}^2 \sin^2 \theta = t$$

Thus the two lowest order amplitudes involve time-like and space-like virtual photons in this case in contrast to e^-e^- scattering in which only space-like $q^2 < 0$ are probed.

A particularly interesting new result during 1969 was the experiments of e^+e^- large angle elastic scattering done at Orsay (5) at $E_{\text{cm}} = \sqrt{s} = 1020 \text{ MeV}$. In this case it was possible to perform an absolute cross section measurement relative to the calculable and measurable rate for γ -rays emitted back-to-back along the beamline from the double bremsstrahlung reaction $e^+e^- \rightarrow e^+e^- + 2\gamma$. The energy spectrum of γ -rays measured for this normalization reaction agreed extremely well with the theoretical spectrum and the luminosity of the colliding beams was determined with only a 0.7% statistical error and a 2.2% systematic error. The cross section for Bhabha scattering integrated over the large solid angles of the detector assemblies of scintillation counters

and spark chambers was found to agree very well with theory as illustrated by the following results

$$\sigma_{\text{exp}} = [1.56 \pm 0.08 \text{ (statistical)} \pm 0.04 \text{ (systematic)}] \times 10^{-31} \text{ cm}^2 \quad 2.9a$$

$$\sigma_{\text{th}} = 1.594 \times 10^{-31} \text{ cm}^2 \quad 2.9b$$

The radiative correction in this case amounted to an 8.3% decrease of σ_{th} for comparison with σ_{exp} . These numbers translate into a limit on a modification of the photon propagator of the form 2.3 which for the 95% confidence result is

$$K > 2.5 \text{ GeV} \quad \text{or} \quad \kappa/K < 10^{-14} \text{ cm} \quad 2.10$$

for either sign of the modification. Since the detectors in this experiment did not distinguish between plus and minus charge of the lepton, the predominant contribution to the cross section was from electrons and positrons continuing into their respective forward hemispheres so that t is smaller than s in 2.8. Thus this measurement is mostly sensitive to modifications of the space-like momentum transfer appearing in the larger amplitude of Fig. 2(b).

For greater sensitivity to the time-like propagator we turn to the process of e^-e^+ annihilation into a muon pair, $\mu^+\mu^-$. In this case there is no longer an amplitude as in Fig. 2(a), so that only the annihilation graph 2(b) contributes. This experiment was also reported from Orsay (5) in 1969. The detection in the case was in the basis of the muons' range in thick plate chambers which allowed them to be distinguished from π 's. The result of this experiment is the most sensitive limit thus far on the photon

propagator in the time-like region with $q^2 = s > 0$. In terms of the 95% confidence criterion, the limit on a modification as in 2.3 is

$$K > 1.3 \text{ GeV} \quad \text{or} \quad \hbar/K < 2 \times 10^{-14} \text{ cm} \quad 2.11$$

In both of these colliding ring experiments one barely begins to probe into the region where couplings of the hadrons with electromagnetism can introduce observable modifications of the predictions of pure QED for an "isolated" electrodynamic system. These modifications appear in the vacuum polarization contribution from hadronic states to the photon propagator as illustrated in Fig. 3.

In general we can summarize them by writing the photon propagator as a mass spectral integral over $\sigma_H(m^2)$, the total annihilation cross section of e^-e^+ pairs of total energy m to hadronic final states, to lowest order in α :

$$\frac{1}{q^2} \rightarrow \frac{1}{q^2} + \frac{1}{4\pi^2\alpha} \int_0^\infty dm^2 \frac{\sigma_H(m^2)}{q^2 - m^2 + i\epsilon} \quad 2.12$$

Since the annihilation cross section is generally of order α^2 this form of correction to the photon propagator is generally two orders of magnitude smaller than expressed in 2.3. In the time-like region of positive q^2 , which is probed in the process of e^+e^- annihilation into $\mu^+\mu^-$ pairs as discussed directly above, there is a large enhancement of σ_H for those values of q^2 coinciding with a resonance. Thus for $q^2 \approx m_\rho^2$ there is an absorptive correction to the propagator

$$1 - \frac{i}{4\pi\alpha} m_\rho^2 \sigma_H(m_\rho^2) \quad 2.13$$

Since this contribution is imaginary it corrects the experimental cross section only by the square factor

$$\left[\frac{m_\rho^2 \sigma_H(m_\rho^2)}{4\pi\alpha} \right]^2 \approx 10^{-3} \quad 2.14$$

which is negligible. Thus the exciting prospect of detecting hadronic contributions--their absorptive as well as dispersive parts--must await analyses of experiments of much higher precision. In particular we shall return to this contribution in analyzing $g-2$, the correction to the Dirac value for the muon's magnetic moment.

A final application of colliding rings for probing QED has been reported during the past year from Novosibirsk where the annihilation of e^-e^+ into 2 γ 's has been measured (6). In this process the virtual particle that is far from its mass shell--i.e. that carries a large four momentum--is not the photon as described in 2.3, but the electron as illustrated in Fig. 4. The preliminary results of this experiment can be summarized by cutting off the fermion propagator in the same way as done for the photon in 2.3. Then with 95% confidence the lower limit on the cut-off is $K = 1.5$ GeV. However an additional theoretical complication is introduced when we study possible cut-off forms for the propagators of charged particles, as in this process, in contrast to a discussion of neutral photons. If we wish to require that a differential law of current conservation should exist at all space-time points, both inside and outside of the interaction region, then we are not at liberty just to modify the propagator of an electrically charged particle. On the contrary, propagator alterations for charged particles require corresponding changes to be imposed on the interaction vertices at which the photons are absorbed and emitted

in order to maintain a charge-current continuity equation at all points (7). The necessary relations between the vertex operators and the electron propagators are expressed in the so-called generalized Ward-Takahashi identities. If we wish to maintain the full content of a differential current conservation law for any modified QED we must honor these identities. Kroll has analyzed the general constraints they impose (8).

Bethe-Heitler processes.--Pair production and bremsstrahlung of muons and electrons at higher energies and with large momentum transfers have been studied during the past decade as probes of QED at small distances (9). As illustrated in Fig. 5 these processes again involve virtual fermion lines bearing space-like four-momenta in the pair production (a) and both space- and time-like four momenta for the two different graphs contributing to the bremsstrahlung (c). The crucial point in using these processes for probing QED is that a target proton, or low Z nucleus (where Born approximation is accurate) can be used to anchor the center of mass system in the laboratory so that large energy and momentum transfers can be accomplished. At the same time the hadron structure can be completely summarized by two invariant electromagnetic form factors and related directly to experimental parameters determined from electron scattering experiments.

Finally the interference between Bethe-Heitler and virtual compton amplitudes (Figs. 5b and 5d) can be removed from the pair production cross section by choosing symmetrical kinematics. In such a symmetric arrangement the cross section is unchanged by interchange of electron and positron. Hence interference of an odd

charge conjugation state of the $e e^-$ pair formed from one photon as produced by the virtual compton amplitude with the even state under C produced by the Bethe-Heitler process (coupling the pair to two photons) will vanish. The small correction to the cross section due to the virtual compton process can thus be reduced to second order and with proper kinematics ignored. Conversely by choosing very asymmetric kinematical conditions its contribution can be emphasized and measured in detail.

In the last two years several new measurements of pair production and bremsstrahlung of muons and electrons have been reported. All are in agreement theory within experimental errors. This includes new measurements of symmetric (10) and asymmetric (11) wide angle electron pair production on carbon at CEA, and from Daresbury (12), the first measurements of wide angle electron pair production on hydrogen. It should also be noted that the total Bethe-Heitler cross section has now been checked to within 1% at energies up to $k = 3.6$ GeV (13).

The results of all the recent high energy experiments are shown in Table 1. Although the method of parameterizing any breakdown of theory is somewhat arbitrary, it turns out as Kroll (8) has shown that a reasonable modification of the pair production and bremsstrahlung amplitude should depend on the second or higher even power of the off shell fermion momentum squared. Accordingly all of these experiments have been parameterized according to

$$\frac{\sigma_{\text{exp}}}{\sigma_{\text{th}}} = (1 \pm m^4/\Lambda^4) \quad 2.15$$

where $m = m_{e^+e^-}$ or $m_{e\gamma}$, etc., is the invariant mass of the final

state. (In the case of symmetric pair production $m_{e^+e^-}^2$ is \approx twice the mass squared of the off shell fermion.) The cutoff limit quoted (14) is the 95% confidence level without considering systematic errors. The sign of the modification has been taken consistently to give the minimum Λ .

Tridents-pair production by leptons.--One can also probe QED at small distances by producing electron or muon pairs by incident electrons or muons, i.e. by producing tridents as illustrated in Fig. 6. Pair production is thus accomplished by virtual photons rather than by real ones as in the Bethe-Heitler process. These measurements have thus far revealed other features of the theory of hadron-photon interactions rather than serving as new probes of pure QED itself. For example, a high energy test of a trident cross section electrons producing muon pairs on carbon has been reported by a Northeastern-CEA group (15). The measurements agree with theory if and only if one allows for interference of the virtual compton amplitude (Fig. 6b) with the time-like photon Bethe-Heitler amplitudes. The results were consistent with the conventional phenomenological model for the compton amplitude based on a diffractively-produced rho decaying into muon pairs. A heavy photon pole of mass less than 400 MeV in the time-like propagator is excluded by this measurement, although this result is dependent on the model for the compton amplitude.

In muon tridents--i.e. production of muon pairs by an incident muon--one has a first direct opportunity to check on the statistics of muons. The analysis of the muon trident experiment carried out at Brookhaven with 11 GeV muons incident on a lead target has now

been completed (16). The observed number of events (89 ± 9.5) agrees well with the theoretical prediction (82 ± 2) for the experimental acceptance geometry. This experiment was sensitive enough to check for the interference of the exchange and direct graphs--theory with interference would predict ~ 113 events.

Further, a depression of the cross section at low pair mass for the like-charged muons due to the exclusion principle has been confirmed. A distinct depression at low invariant pair mass for Fermi-Dirac particles occurs since the two identical muons have similar directions and energies and therefore similar wave functions. The muon thus appears to be a fermion.

Finally to conclude this section we note that the Born diagrams of QED have been directly confronted by experiment. For anyone looking for that elusive sign of breakdown of the theory at momentum transfers of the order of a nucleon mass, there can be no joy. All the combinations of virtual electron, muon, and photon propagators and vertices have been checked; the possible cutoffs have been pushed to 1 GeV or higher. Figure 7 summarizes the situation using 2.3 and 2.15 to modify the propagators. There remains for us at this stage only to look for any evidence of differences between the muon and electron that may reveal themselves in these high energy probes.

Electron-muon universality.--We have as yet no clue as to the difference between electrons and muons aside from their large mass ratio. As discussed above the wide angle pair production bremsstrahlung and trident experiments have yielded results consistent with QED for both muons and electrons. Thus for large space-like as well as

time-like momenta they show the same behaviors. What then is the origin of their large mass difference? Might this mass difference indicate that their structures are different, or that there are special couplings for muons and not electrons, or vice versa? Although there was no evidence of this sort in the high q -experiments reviewed above, can we probe further the universality of muon and electron interactions by other experiments?

One direct possibility is to study the ratio of muon to electron scattering for evidence of a difference in structure. This applies both to elastic and inelastic scattering at high energies where we can work in Born approximation for scattering from proton or light Z targets, and where finite muon mass corrections are also small.

The ratio of μ - p to e - p elastic scattering has been checked most thoroughly in a recent Brookhaven experiment (17) to be independent of q^2 throughout the range of $0.15 < |q^2| < 0.9$ $(\text{GeV}/c)^2$. The measurements included negative muons up to 17 GeV/c incident momenta and positive muons up to 11 GeV/c . Although their ratio to e - p scattering is q^2 -independent, the μ - p cross sections lie 8% below the e - p ones. The authors have found it difficult to account for this difference; the main experimental uncertainties are systematic: a 4% uncertainty in the cross sections from the determination of q^2 and a 2% one in the normalization. Discounting the possibility of a normalization error and fitting the cross section ratio in terms of a form factor at the electron and muon vertices of the form

$$\frac{G_{\mu}(q^2)}{G_E(q^2)} = \frac{1}{1 + q^2 \left[\frac{1}{\Lambda_{\mu}^2} - \frac{1}{\Lambda_e^2} \right]}, \quad 2.16$$

their results imply to 95% confidence

$$\frac{1}{\Lambda^2} \equiv \left| \frac{1}{\Lambda_{\mu}^2} - \frac{1}{\Lambda_e^2} \right| = (2.26 \text{ GeV}/c)^{-2}, \quad 2.17$$

corresponding to a mean square radius difference

$$\Delta \langle r^2 \rangle \equiv \frac{6}{\Lambda^2} \sim (2.1 \times 10^{-14} \text{ cm})^2. \quad 2.18$$

Electron-muon universality can also be checked for coupling to time-like photons from the decay branching ratios of vector mesons into e^+e^- versus $\mu^+\mu^-$. Considerable caution should be taken in combining colliding beam and photoproduction data since the $\rho\omega$ and $\rho\omega\phi$ interference problems are very complicated and the definitions of the resonance spectra are different (18). The following results show what has been learned by this approach.

For the ρ meson the branching ratios are (16,18)

$$\frac{\Gamma(\rho \rightarrow \mu^+\mu^-)}{\Gamma(\rho \rightarrow \text{all})} = (7.9 \pm 2.0) \times 10^{-5} \quad 2.19$$

and (19)

$$\frac{\Gamma(\rho \rightarrow e^+e^-)}{\Gamma(\rho \rightarrow \text{all})} = (6.5 \pm 1.4) \times 10^{-5} \quad 2.20$$

from photoproduction experiments, and

$$\frac{\Gamma(\rho \rightarrow e^+e^-)}{\Gamma(\rho \rightarrow \text{all})} = (5.9 \pm 0.7) \times 10^{-5} \quad 2.21$$

from an average of colliding beam measurements (20,21).

Preliminary results for the branching ratio of photoproduced ϕ into muon pairs has been reported by groups from Northeastern (18) and Cornell (22)

$$\frac{\Gamma(\phi \rightarrow \mu^+ \mu^-)}{\Gamma(\phi \rightarrow \text{all})} = \begin{cases} (2.34 \pm 1.01) \times 10^{-4} & \text{Northeastern} \\ (2.1 \pm 0.3) \times 10^{-4} & \text{Cornell (preliminary} \\ & \text{statistical error only)} \end{cases} \quad 2.22$$

These results may be compared with the DESY-MIT (23) measurement of the e^+e^- branching ratio (from photoproduction of ϕ 's)

$$\frac{\Gamma(\phi \rightarrow e^+ e^-)}{\Gamma(\phi \rightarrow \text{all})} = (2.9 \pm 0.8) \times 10^{-4} \quad 2.23$$

and a new result from colliding beam measurements at Orsay (5,24)

$$\frac{\Gamma(\phi \rightarrow e^+ e^-)}{\Gamma(\phi \rightarrow \text{all})} = (3.73 \pm 0.25) \times 10^{-4} \quad 2.24$$

Further experiments are obviously required here, especially a simultaneous measurement of the e^+e^- and $\mu^+\mu^-$ decay modes.

Finally we record that all other attempts to uncover strange interactions of the muon or electron have also failed. Electrons could conceivably couple to heavy leptons via current conserving magnetic moment couplings as suggested by Low (25,26). However searches (27,28,29,30) for a heavy lepton in the reaction

$$e + p \rightarrow e^* + p \rightarrow e + \gamma + p \quad 2.25$$

have given negative results for m_{e^*} in the range 100 MeV to 1300 MeV. This is of course consistent with the lack of deviation from ordinary theory in the wide angle electron pair and bremsstrahlung experiments. For the muon there are also new and more stringent limits on the conservation of muons in analogy with electron conservation. Thus there is now a limit on its radiative conversion

into an electron (31,32)

$$\frac{\Gamma(\mu \rightarrow e\gamma)}{\Gamma(\mu \rightarrow e\nu\bar{\nu})} < 0.6 \times 10^{-8} \quad 2.26$$

If this conservation law were multiplicative, the reaction

$$e^-e^- \rightarrow \mu^-\mu^- \quad 2.27$$

would be possible. An upper limit on the cross section has been established at the Stanford storage ring (33)

$$\sigma < 0.67 \times 10^{-32} \text{ cm}^2 \text{ (95\% conf)}. \quad 2.28$$

3. PRECISION TESTS OF QUANTUM ELECTRODYNAMICS

The fine structure constant.--Although high momentum transfer tests are essential for detecting possible new interactions or deviations at short distances, they are, as we have seen, only sensitive to Born diagrams. Tests of the high order corrections, including those involving renormalization effects require the very high precision atomic hyperfine and fine structure measurements and precise determinations of the electron and muon anomalous magnetic moments. In particular, the Lamb shift measurements are sensitive to the dynamical effects of quantum electrodynamics through fourth order in perturbation theory, as well as relativistic recoil corrections which emerge from the covariant treatment of the hydrogen atom bound state. The measurements of the magnetic moment of the electron are on the threshold of checking quantum electrodynamics through sixth order in perturbation theory. Moreover, at the level of precision now possible in studying the muon's $g-2$ value, one is able to probe the effect in an isolated electrodynamic system of very interesting hadronic and weak interaction contributions buried in the vacuum polarization. Thus, as we shall see, it is possible to infer limit on the e^+e^- annihilation cross section into the entire spectrum of hadrons from measurements of the muon moment. In addition, statements about the polarizability of the proton structure itself can be inferred from the fantastically precise measurements of the ground state hyperfine splitting of hydrogen.

The remaining goal of the atomic physics tests is aesthetic;

the hydrogen atom is the fundamental two-body system and perhaps the most important tool of physics; 57 years after the Bohr theory the challenge is still there to calculate its properties to the highest accuracy possible.

This is an excellent time to review the progress of the precision tests, since at present there are no outstanding discrepancies between theory and experiment. In addition to a great deal of new experimental results for energy levels of hydrogenic atoms, the massive new analysis of the data relevant to the determination of the fundamental constants by Taylor, Parker and Langenberg (34) has provided a new and precise set of values for the 1970's. For the first time, the value of the fine structure constant $\alpha = e^2/4\pi\hbar c$, upon which many of the precision tests of QED hinge, can be determined to high accuracy from experiments totally independent of QED input. The most precise determination is obtained from a combination of measurements from very diverse fields, expressed via the relation (34)

$$\alpha^{-2} = \frac{1}{4Ry_{\infty}} \frac{1}{\gamma_p} \frac{\mu_{p'}}{\mu_B} \frac{2e}{h} \frac{c\Omega_{abs}}{\Omega_{NBS}}, \quad 3.1$$

where the Rydberg Ry_{∞} , the proton gyromagnetic ratio in water γ_p , the magnetic moment $\mu_{p'}/\mu_B$ of the proton (in a water sample) in units of the electron Bohr magneton, and $c\Omega_{abs}/\Omega_{NBS}$ the ratio of absolute to NBS ohm (required for standard voltage measurements) are known to one or two parts per million, and the ratio $2e/h$ has been determined to better than 1 ppm via the A. C. Josephson effect in superconductors by Parker, Taylor, and Langenberg (35)² and later work by Finnegan, Denenstein, and Langenberg (36).

The result of the least square ^{adjustment} Λ of Taylor et al. (34) is

$$\alpha^{-1} = 137.03608 \pm 0.00026 \text{ (1.9 ppm) } , \quad 3.2$$

a value which, as 3.1 makes clear, does not rely on any measurement dependent on QED. Thus, finally with this new and more precise value of α , all of the input constants necessary for comparing theory and experiment are known sufficiently to permit critical and much less ambiguous tests of theory.³

Another extremely valuable contribution of Taylor et al. (35) is their complete and careful reassessment of the accuracy of the atomic physics tests of QED; critical and uniform criteria (based on statistical and systematic errors) are given for the evaluation of the one standard deviation limits of the various energy level measurements. This now allows a confrontation of theory and experiment which does not rely on vague and inconsistent comparisons based on "limits of error". In our review, we shall adopt the Taylor et al. assignment of the one standard deviation error; typically their value was about two-thirds of the "limit of error" assigned by the experimentalists.

The anomalous magnetic moment of the electron.--The direct, basic test of QED is the anomalous magnetic moment $a_e = (g-2)/2$ of the electron. Thus far, it has been one of the most stunning triumphs of theoretical analysis. Measurements of the g-value to a precision of a few parts in 10^9 have been possible due to the wonderful fact that in a static uniform field the spin and momentum vectors of a particle of spin $1/2$ and unit magnetic moment--i.e. a g-value of exactly 2--retain a constant relative direction angle.

It is thus possible to determine $g-2$ directly by measuring the precession of spin relative to the momentum as determined from the Mott scattering pattern for electrons impinging on a scattering foil.

In the experiment of Wilkinson and Crane (40), a beam of polarized electrons are trapped in a solenoidal magnetic field between magnetic mirrors. The final result for a_e derived from the Michigan data [including corrections by Rich (41) for the computation of the mean field B , and revisions of the relativistic pitch corrections (required because the electron orbit is not exactly in a plane perpendicular to B) by Henry and Silver (42)] is

$$a_{e^-}^{\text{exp}} = 0.001\ 159\ 549(30) \quad 3.3$$

The same basic experimental technique has also been used recently by Gilleland and Rich (43) to measure the magnetic moment of the positron. Their result is

$$a_{e^+}^{\text{exp}} = 0.001\ 160\ 200(1100) \quad 3.4$$

which verifies to 1 ppm the CPT statement that the electron and positron g factors are equal.

Very recently Rich and co-workers (44) have performed a new measurement of a_{e^-} and obtained a result which differs significantly from 3.3 :

$$a_{e^-}^{\text{exp}} = 0.001\ 159\ 646(7) \quad 3.5$$

As we shall see, this new result is quite consistent with present theoretical calculations.

A particularly promising new radio frequency resonance method

for measuring a_e has been developed by groups at Bonn (45) and the University of Washington (46). Circulating electrons (with polarization parallel to B), subjected to a perturbing field of frequency $\omega_{\text{spin}} = \frac{1}{2} g(e/mc)B$ will be spin-flipped and depolarized. Spin-flip also occurs if the frequency $\omega_a = a(e/mc)B$ is applied because the electron, in its rest frame, sees ω_a combined with the cyclotron frequency $\omega_c = (e/mc)B$, again giving the depolarizing frequency ω_{spin} . The determination of the resonance frequencies ω_a and ω_c then yields a_e . The result reported thus far from the Bonn group (45) is

$$a_{e^-}^{\text{exp}} = 0.001\,159\,660(300) ; \quad 3.6$$

the 1σ error is expected to be greatly reduced in the future.

Anomalous moment (theory).--As in the case for all spin 1/2 particles, the electron's interactions with an external electromagnetic field are completely specified by the Dirac and Pauli form factors defined by the matrix element of the current:

$$e\bar{u}(p+q) \left[\gamma_\mu F_1(q^2) + \frac{i\sigma_{\mu\nu}q_\nu}{2m} F_2(q^2) \right] u(p) \quad 3.7$$

This is the most general form allowed on the basis of current and parity conservation (47). For static magnetic fields this expression leads to the usual electron Larmor and spin interaction terms $e/2m \underline{L} \cdot \underline{H}$ and $e/2mg \underline{S} \cdot \underline{H}$, where $eF_1(0) = e$ corresponds to the definition of the electron charge and $g(1+a) = 2(1+F_2(0))$ is the total g-factor. On the other hand the behavior of F_1 and F_2 for $q^2 \neq 0$ corresponds to a spatial distribution of charge and magnetic moment. This modifies the Coulomb and hyperfine

interactions in hydrogenic atoms and is essentially what is tested in the level shift measurement discussed in the later sections.⁴ QED completely specifies these form factors; their deviation from pure Dirac point-like behavior is calculable in perturbation theory from the rules and renormalization techniques developed by Feynman, Schwinger, and others (1).

The present theoretical prediction for the electron moment is

$$F_2(0)_e = a_e^{\text{th}} = \frac{1}{2} (\alpha/\pi) - 0.32848 (\alpha^2/\pi^2) + 0.55 (\alpha^3/\pi^3) \quad 3.8$$

The first term is the famous result obtained by Schwinger in 1948 (49). The fourth order radiative corrections were calculated by Karplus and Kroll (50) (who were the first to demonstrate the consistency of the renormalization procedure in fourth order) and later corrected by Sommerfield (51) and Petermann (52). In Sommerfield's compact method, which is probably the most useful for extension to higher orders, the fourth order self-energy correction to a bound state electron is computed in the Furry picture and then expanded to first order in the magnetic field. More recently, the fourth order correction has been computed via dispersion theory by Terentev (53).

The sixth order coefficient in 3.8 consists of (a) the contribution (0.13) from the Drell-Pagels-Parsons (54,55) dispersion theory estimate of the three-photon radiative corrections, (b) a contribution (0.055) by Mignaco and Remiddi (56) for the contribution of fourth order vacuum polarization to the sixth order moment, and (c) the contribution 0.36 ± 0.04 from photon-photon scattering sub-diagrams evaluated numerically by Aldins, Brodsky, Dufner, and

Kinoshita (57). (The α^3/π^3 contribution from second order vacuum polarization insertions into the fourth order vertex have not yet been calculated.)

The exact calculation of sixth order radiative corrections to the lepton vertex is obviously a horrendous task. There are two central problems: (1) the reduction of matrix elements with three loop integrations to Feynman parametric form and (2) the multi-dimensional integration of the resulting integrand. In the photon-photon scattering contribution calculation of Aldins et al. (57), all the trace algebra and substitutions required to accomplish step (1) were performed automatically using an algebraic computation program written by Hearn (58). The resulting 7-dimensional integration was performed numerically using a program which on successive iterations improves the Riemann integration grid through a random variable sampling technique. A similar calculation of the three-photon correction to the electron vertex would be considerably more difficult but not out of the question.

Although it does not eliminate the necessity for a full calculation of the sixth order moment, the estimate of Drell et al. (54,55) strongly suggests that the final result for the three photon corrections will be positive and numerically small. In this method, a_e is computed from a "sidewise" dispersion relation in the mass of one of the lepton lines entering the electromagnetic vertex, but in the approximation that the absorptive amplitude is dominated by the threshold dependence of the electron-one photon intermediate state illustrated in Fig. 8. The required Compton amplitude is exactly determined in this region by the low energy

theorem, which again involves the anomalous moment. The self-consistent solution for a_e was found to give good results for the second and fourth order contributions to the electron and muon moments and provided the estimate $0.13 \alpha^3/\pi^3$ for the sixth order term. The main uncertainty in this sixth order estimate comes from the neglect of multiparticle cut contribution to the absorptive amplitudes, although as shown by Parsons (55) they do not contribute to the limiting threshold behavior.

Theory and experiment are most easily compared if we write the experimental Wilkinson-Crane-Rich result 3.3 in the form [$\alpha^{-1} = 137.03608(26)$]

$$a_{e^-}^{\text{exp}} = \frac{1}{2} (\alpha/\pi) - 0.3285 (\alpha/\pi)^2 - (7.0 \pm 2.4) (\alpha/\pi)^3 \quad 3.9$$

On the other hand, the new result 3.5 of Rich and his co-workers is (39)

$$a_{e^-}^{\text{exp}} = \frac{1}{2} (\alpha/\pi) - 0.3285 (\alpha/\pi)^2 + (0.54 \pm 0.55) (\alpha/\pi)^3 \quad 3.10$$

which is very consistent with the present indicated sign and magnitude of the sixth order theoretical coefficient. Further experiments and further development of the theoretical result will be required before we can be confident that QED is confirmed through sixth order in perturbation theory. The remarkable fact is that for the total moment $g = 2(1+a)$, theory and experiment appear to agree in the eighth (and possibly ninth) significant figure.

The muon anomalous moment (experimental).--Over the last few years increasingly accurate measurements of the anomalous magnetic moment of the muon have been performed at CERN (59). The principle of the experiment is the same as that of the Wilkinson-Crane electron measurement, although the muon is conveniently born fully polarized (in $\pi \rightarrow \mu + \nu$ decay) and readily shows its final polarization through the asymmetry of the $\mu \rightarrow e + 2\nu$ decay (maximum along the μ spin). The short muon lifetime ($2.2 \mu\text{sec}$) is dilated to $27 \mu\text{sec}$ using highly relativistic (1.2 GeV) muons, thus increasing the number of anomalous precession cycles available for study. In the CERN experiments, the polarized muons are injected into and stored in a 5-meter storage ring. The counting rate for the forward decay electrons shows a modulation at the $g-2$ precession frequency $\omega_a = a_\mu (e/m_\mu) B$. (See Fig. 9.) The most recent result (59,60) which includes both μ^+ and μ^- measurements is

$$a_\mu^{\text{exp}} = 0.001\,166\,16(31). \quad (1\sigma) \quad 3.11$$

Although the experimental error (from statistical and effective magnetic field uncertainties) is 40 times larger than the best corresponding electron result, it is, in fact, only 7% of the theoretical $(\alpha/\pi)^2$ result and is comparable in size with the light-by-light scattering contribution to the muon moment.

Theoretical prediction for a_μ .--If we assume electrons and muons have the same electrodynamic couplings, all of the Feynman graphs which contribute to the electron moment contribute equally to that of the muon. In addition, electron loop insertions in the muon vertex give additional QED contributions to a_μ , enhanced by

factors of $\log m_\mu/m_e$:

$$\Delta a_\mu (\text{elec. vac. pol}) = \frac{1}{3} \left(\frac{\alpha}{\pi} \right)^2 \left\{ \log \frac{m_\mu}{m_e} - \frac{25}{12} + \frac{3\pi^2}{4} \frac{m_e}{m_\mu} + 3(3 - 4 \log \frac{m_\mu}{m_e}) \frac{m_e^2}{m_\mu^2} + o\left(\frac{m_e^3}{m_\mu^3}\right) \right\} \quad (61-63)$$

$$+ \left(\frac{\alpha}{\pi} \right)^3 \left\{ \frac{2}{9} \log^2 \frac{m_\mu}{m_e} - 1.114 \log \frac{m_\mu}{m_e} + 2.44 \pm 0.5 \right\} \quad (64-66)$$

$$= (1.0943) \left(\frac{\alpha}{\pi} \right)^2 + (2.82 \pm 0.5) \left(\frac{\alpha}{\pi} \right)^3.$$

3.12

The corresponding muon loop contribution to the electron moment, $\alpha^2/(45\pi^2) m_e^2/m_\mu^2$, is negligible (66). Several terms which contribute to the non-logarithmic α^3/π^3 contribution in 3.12 have only been estimated (65). The limits correspond to an upper error limit for this estimate. The electron loop contribution to the muon moment from sixth order diagrams containing photon-photon scattering subdiagrams turns out to be surprisingly large (57), (see Figure 10)

$$\Delta a_\mu (\text{photon-photon}) = (18.4 \pm 1.1) \alpha^3/\pi^3, \quad 3.13$$

due to a logarithmic dependence $[(6.4 \pm 0.1) \log m_\mu/m_e + \text{const}] \alpha^3/\pi^3$ on the electron mass for $m_\mu/m_e \gg 1$. The error limits represent the uncertainty in the required numerical integrations (over 7 and 5 dimensions, respectively). With the inclusion of the photon-photon scattering contribution all of the Feynman diagrams from QED which contribute to the difference of a_μ and a_e have now either been calculated or carefully estimated through sixth order.

The non-electrodynamic contributions to the muon moment are of

very much theoretical interest in their own right. Their contribution to the muon g -value is very much larger than to the electron's $g-2$ since the muon's greater mass means that one is probing with much higher momenta and hence at smaller distances in the closed loops in the Feynman graphs. For the muon case these momenta become comparable to the masses of important hadron states. The hadronic contribution to a_μ [due to vacuum polarization insertions in the second order vertex] may be related to the annihilation cross section measured in the colliding beam experiments (see Fig. 11)

$$\Delta a_\mu \text{ (hadronic)} = \frac{1}{4\pi^3} \int_{4m_\pi^2}^{\infty} ds \sigma_{e^+e^- \rightarrow \text{hadrons}}(s) G(s) \quad 3.14$$

where

$$G(s) = \int_0^1 dz \frac{z^2(1-z)}{z^2 + (1-z)s/m_\mu^2} .$$

The current Orsay measurements (67) for the e^+e^- annihilation cross section in the region of $s \sim m_\rho^2, m_\omega^2, m_\phi^2$ yield the respective contributions (68)

$$\begin{aligned} \Delta a_\mu \text{ (hadronic)} &= [5.4 \pm 0.3 + 0.61 \pm 0.12 + 0.50 \pm 0.08] \times 10^{-8} \\ &= [6.5 \pm 0.5] \times 10^{-8} \end{aligned} \quad 3.15$$

Until there are further $\sigma_{e^+e^-}$ measurements, the contribution to Δa_μ from hadrons beyond the ϕ is open to speculation (69,70). A recent analysis by Bell and deRafael (71) shows that even the current-field identity approach to the electromagnetic interactions does not give a useful bound for Δa_μ (hadronic) unless a strict

vector dominance model is assumed. Equation 3.15 also shows why this contribution is more important by roughly a factor of $(m_\mu/m_e)^2$ for the muon relative to the electron g-value.

Even more speculative is the contribution of weak interactions to a_μ . If intermediate boson W is assumed to exist, it modifies the muon vertex and contributes (72-74)

$$\Delta a_\mu(\text{weak}) = \frac{G_F M_N^2}{8\pi^2 \sqrt{2}} [2(1 - \kappa_W) \log \xi + 10/3] ; \quad 3.16$$

$G_F \cong 10^{-5}/M_N^2$ is the Fermi constant (independent of the W mass). Here κ_W is the anomalous moment of the spin-one boson and $\xi \sim M_W^2/\Lambda^2 \rightarrow 0$ is a gauge-invariant regulator of an ultraviolet divergence. Lee (75) has proposed that when radiative corrections to this result are included, $\Delta a_\mu(\text{weak})$ will become finite for $\xi \rightarrow 0$. With this assumption and $\kappa_W = 0$, $\log \xi \rightarrow \log \alpha$ and $\Delta a_\mu(\text{weak}) \sim -1.0 \times 10^{-8} \sim 0.8 (\alpha/\pi)^3$, which is 1/30 of the present experimental error. Other prescriptions, such as a unitarity bound for Λ^2 give a similar correction. On the other hand, since this weak interaction contribution is of the "diagonal" type (76), it may not be related to the usual weak interactions, and the above estimates may be unreliable.

The total theoretical prediction is then (57)

$$\begin{aligned} a_\mu^{\text{th}} &= \frac{1}{2} \alpha/\pi + 0.7658 \alpha^2/\pi^2 + (27 \pm 3) \alpha^3/\pi^3 \\ &= 0.00116587 (3) \end{aligned} \quad 3.17$$

where we have not included any uncertainty from the sixth order result for a_e , hadron vacuum polarization beyond $s = m_\phi^2$, or the cut-off dependent weak interaction contribution. Comparing this

with 3.11, we find theory and experiment agree to within one standard deviation:

$$a_{\mu}^{\text{exp}} - a_{\mu}^{\text{th}} = (29 \pm 34) \times 10^{-8} = (250 \pm 290) \text{ ppm}, \quad 3.18$$

which is a remarkable success for the application of QED to the muon. If we wish, we can use the above agreement for a_{μ} to rule out (to 90% confidence) (a) negative metric photons or photon-propagator cutoffs of mass less than 5 GeV, (b) new vector fields coupled to the muon with coupling to mass ratio f^2/m^2 greater than $6 \times 10^{-4}/m_{\mu}^2$ (77), (c) additional leptons with mass less than $30 m_e$. In addition, the present agreement of theory and experiment bounds the electron-positron annihilation cross section integrated over the entire hadronic spectrum (57):

$$\int_{s > m_{\phi}^2}^{\infty} \frac{\sigma_{e^+e^-}(s)}{s} < 8.2 \mu\text{b} \quad 3.19$$

i.e. the contribution of all hadrons to a_{μ} is not more than three or four times that of the ρ . The implications of the agreement between the theory and experimental values for the muon moment for various speculative theories has been summarized by Bailey and Picasso (78). Clearly a reduction in the experimental error would not only further check the QED corrections but also would provide information in important questions of the strong and weak interactions.

Atomic physics tests of QED--The Lamb shift.--The historic tests of QED have been the energy levels of the hydrogen atom, the fundamental two body system. [See Fig. 12.] More recently,

this testing ground has been extended to other hydrogenic atoms including positronium and muonium for which the complications of hadron dynamics are more remote.⁵ The dynamics of these atoms are specified by the interaction density of QED, $H_I = e: \bar{\psi} \gamma_\mu \psi A^\mu$, plus the Maxwell and Dirac equations, as expressed in perturbation theory in the form of the Feynman rules. The theoretical setting for the computation of the bound states of the hydrogenic atom is the Bethe-Salpeter equation (78-81). If the atomic level experiments are idealized as photoabsorption measurements, then as shown by Low (82) the line centers of the absorption spectra are determined by the eigenvalues of the full B-S equation to at least order α^3 .

The typical (irreducible) kernels which must be considered for the hydrogen atom are shown in Fig. 13. The one photon exchange kernel upon iteration corresponds to the sum of all "ladder" graphs for electron-proton scattering. It can be shown (83-85) that the B-S equation reduces properly to the Dirac equation when $m_e/m_p \rightarrow 0$, if and only if all crossed graph kernels are included.

The dominant interactions of the atom, the Coulomb potential $-Z\alpha/r$ can be separated off from the rest of the electrodynamic interaction most readily if we use the radiation gauge in the atomic center-of-mass system. The Coulomb interaction, which must be treated to all orders in perturbation theory, can then be separated out from the Feynman propagator for exchanged photons. The remainder describes the transverse (Breit) interaction

$$iD_F^{\text{tr}}(q)_{\mu\nu} = \frac{-ig_{\mu\nu}}{q^2 + i\epsilon} - i \frac{\delta_{\mu 0} \delta_{\nu 0}}{|q|^2} \quad 3.20$$

The famous degeneracy of the $2P_{1/2}$ and $2S_{1/2}$ levels in the Dirac theory is rather delicate (and peculiar to one electron atoms) since it is removed by any modification of the Coulomb interaction (including shielding due to the presence of other orbital electrons). In particular, modifications occur from (non-reduced mass) recoil corrections, the finite nuclear size R_N , vacuum polarization, as well as the most important contribution to the level shift, the self-energy correction to the bound electron. The various contributing terms can be classified in terms of the available small parameters, α , m_e/M_N , $Z\alpha$, and $Z\alpha m_e R_N = R_N/a_0$ where $Z\alpha$ indicates the dependence on the strength of the Coulomb potential, and R_N/a_0 is the nuclear radius in units of the Bohr radius. The theoretical formula for the $2S_{1/2}$ - $2P_{1/2}$ separation (Lamb shift) indeed takes the form ($m =$ reduced mass; $h = c = 1$)

$$\begin{aligned} \Delta E_n(2S_{1/2}-2P_{1/2}) &= \alpha(Z\alpha)^4 m [a_1 \log Z\alpha + a_0] + \alpha(Z\alpha)^5 m [b_0] \\ &+ \alpha(Z\alpha)^6 m [c_2 \log^2 Z\alpha + c_1 \log Z\alpha + c_0] + \alpha^2(Z\alpha)^4 m [d_0] \\ &+ m/M_N (Z\alpha)^5 m [e_1 \log Z\alpha + e_0] + (Z\alpha)^4 (mR_p)^2 [f_0] \end{aligned} \quad 3.21$$

plus terms of 7th and higher order in the small parameters. The a_0 terms are of order $\alpha(Z\alpha)^2$ relative to the basic binding unit, the Rydberg, $Ry_\infty = \frac{1}{2} (Z\alpha)^2 m$.

Radiative corrections. -- Numerically, the dominant contribution to the Lamb shift is the radiative correction due to the emission and subsequent reabsorption of a photon of the bound electron [Fig. 13c]. The a_1 term in 3.21 can be evaluated non-relativistically

from second order perturbation theory in the transverse interaction:⁶

$$\Delta E_n = \frac{e^2}{(2\pi)^3} \int \frac{d^3k}{2k} \sum_m \sum_{\lambda=1,2} \frac{\langle n | \mathbf{j}_e \cdot \boldsymbol{\epsilon}_\lambda e^{-ik \cdot \mathbf{x}_e} | m \rangle \langle m | \mathbf{j}_e \cdot \boldsymbol{\epsilon}_\lambda e^{-ik \cdot \mathbf{x}_e} | n \rangle}{E_n - E_m - k + i\epsilon} \quad 3.22$$

as in the historic calculation by Bethe in 1948 (86). Part of ΔE_n survives even if the binding potential is turned off: this contribution (obtained by neglecting $E_m - E_n$ in the denominator) shifts all levels equally and can be incorporated into the definition of the mass of the free electron. Thus the dependence of the correction on the individual bound states is what is observed as an experimental shift between different levels. This was the original stimulus toward a renormalized and covariant theory of quantum electrodynamics (1).

From a physical point of view, the energy shift 3.22 is a consequence of the zero point fluctuations, and hence non-vanishing values of the mean square electric and magnetic field strengths (E and B are not mutually commuting or simultaneously measurable observables). Under the influence of these fluctuations, the electron charge is effectively spread over a mean square radius (87)

$$\langle r^2 \rangle \sim m^2 Z\alpha/\pi \log(Z\alpha)^{-1} \sim (5 \times 10^{-12} \text{ cm})^2 \text{ for } Z = 1, \quad 3.23$$

which weakens the $-Z\alpha/r$ binding and shifts s-states upward by $\Delta E_n \sim \alpha(Z\alpha)^2 \log(Z\alpha)^{-1} \text{ Ry}$. The imaginary part of ΔE_n gives the decay rate of state n via one photon emission.

When the self-coulomb interaction of the bound electron is

included, the relativistic result for the lowest order a_0 and a_1 terms is (88)

$$\Delta E_n = \frac{-2\alpha}{3\pi m^2} \langle n | \underline{p} \left[\log \frac{m/2}{(H_{NR} - \epsilon_n)} + \frac{11}{24} \right] \underline{p}, e\mathcal{A} | n \rangle + \frac{\alpha}{2\pi} \left(-\frac{e}{2m} \right) \langle n | \frac{1}{2} \sigma_{\mu\nu} F^{\mu\nu} | n \rangle + \Delta E_{vp} \quad 3.24$$

$$\text{Re } \Delta E_n = \frac{4}{3\pi} \frac{\alpha (Z\alpha)^4 m}{n^3} \begin{cases} \log \frac{1}{(Z\alpha)^2} + \log \frac{(Z\alpha)^2 m}{2 |\epsilon_n - \epsilon_{n'}|_{av}} + \frac{11}{24} + \frac{3}{8} - \frac{1}{5} & (\text{S-states}) \\ \log \frac{(Z\alpha)^2 m}{2 |\epsilon_n - \epsilon_{n'}|_{av}} + \frac{3}{8} \frac{C_{\ell j}}{2\ell+1} & (\text{non-S-states}) \end{cases} \quad 3.25$$

where $C_{\ell j} = (\ell+1)^{-1}$ for $j = \ell + 1/2$ and $-\ell^{-1}$ for $j = \ell - 1/2$ and m is the reduced mass. The first two lines show the resemblance of the bound electron current to that of the free vertex (see 3.7). The $\log(H_{NR} - \epsilon_n)$ term demonstrates how binding corrections eliminate what was an infrared divergence in the free vertex, and accounts for the $\log(Z\alpha)$ behavior of the final result. Physically, the self-energy photons of wavelength larger than atomic distances contribute equally to the bound and free electron and do not contribute to ΔE_n . This term and the required values of $|\epsilon_n - \epsilon_{n'}|_{av}$ [~ 16.64 Ry for the $2S_{1/2}$ level] can be evaluated by Bethe's sum-on-states method or by algebraic-numerical techniques (89-91). The $3/8$ terms are from the $\underline{\alpha} \cdot \underline{\epsilon}$ terms of the $\alpha/2\pi$ anomalous moment $\sigma_{\mu\nu} F^{\mu\nu}$ contribution. The $-\frac{1}{5}$ term is the lowest order Serber (92)-

Uehling (93) vacuum polarization contribution due to the modification of the Coulomb interaction from virtual pairs:

$$-\frac{Z\alpha}{r} \rightarrow -\frac{Z\alpha}{r} - \frac{Z\alpha}{r} \int_{4m_e^2} ds \frac{\pi(s)}{s} e^{-\sqrt{s} r} \quad 3.26$$

The weight function $\pi(s)/s = \sigma_{e^+e^-}(s)/4\pi^2\alpha$ is the e^+e^- annihilation cross section and includes contributions from all charged pairs although only electron pairs are important in practice. Note that in the classical limit ($r \rightarrow \infty$) which defines the units of charge, the coulomb potential is unmodified. For $r \lesssim m_e^{-1} \approx 10^{-11}$ cm, the electron penetrates the shielding cloud of virtual pairs and sees a proton potential more attractive than the pure coulomb result, lowering S-state energy levels, in contrast to the self-energy radiative corrections which weaken the binding.

The contribution from 3.25 to the $2S_{1/2}-2P_{1/2}$ separation in H is 1051 MHz, including -27 MHz from the vacuum polarization correction. The comparison with experiment is sensitive to the contribution of terms of order 0.1 MHz, and thus requires the evaluation of the second order in α radiative corrections (i.e. the d_0 terms) as well as contributions through order $\alpha(Z\alpha)^6 m$ from higher order binding and relativistic wave function corrections. As is so often the case when the Coulomb potential is involved, any expansion in powers of the binding potential must be handled with great care. Note the $\log Z\alpha$ dependence of the result in 3.25. These are the clear tip off that care and delicacy are required in the expansion.

Considerable progress in the technical problems has been made over the years by many workers [see Erickson and Yennie (94) for a complete review]. The most systematic method has been given by Erickson and Yennie (94), who not only systematically verified previous calculations of order $\alpha(Z\alpha)^5 m$, $\alpha(Z\alpha)^6 m \log^2 Z\alpha$, and $\alpha(Z\alpha)^6 m \log Z\alpha$, but also obtained the dominant contribution to order $\alpha(Z\alpha)^6 m$. In their method one starts from the covariant expression for the self-energy shift of the bound electron⁷

$$[(\not{\pi}-m)|n\rangle = 0, \pi^\mu = (E_n + Z\alpha/r, \mathbf{p}), m_e/m_p \rightarrow 0]$$

$$\Delta E_n^{\text{SE}} = \frac{e^2}{(2\pi)^4} \int \frac{d^4 k/i}{k^2+i\epsilon} \langle \bar{n} | \gamma_\mu \frac{1}{\not{\pi}-\not{k}-m+i\epsilon} \gamma^\mu | n \rangle - \langle \bar{n} | \delta m | n \rangle \quad 3.27$$

The Feynman calculation of the self-energy shift for the free electron is then used as a guide for the corresponding calculation for a bound electron. The calculation of the bound and free case would be identical and the result $\Delta E_n^{\text{SE}} = 0$ would be obtained if it were not for the fact that the components of π_μ do not commute with each other. Remainder terms are those which are at least linear in the commutator $[\pi_\mu, \pi_\nu] = -ie F_{\mu\nu} = -ie[\partial_\mu A_\nu - \partial_\nu A_\mu]$. Thus the expansion is in terms of the gauge invariant field strength $F_{\mu\nu}$ rather than the potential A_ν ; spurious gauge-dependent terms do not arise (95). The calculations are greatly systematized by the development of a simple "rule of order" which quickly identifies the order of magnitude (powers of $Z\alpha$) of a given term. Thus it is found sufficient to retain only terms explicitly linear or quadratic in $F_{\mu\nu}$ [binding corrections in the denominators, however, need to be retained to avoid artificial infrared divergences as in 3.21, 3.25].

The comparison with experiment also requires the evaluation of fourth-order radiative correction (two virtual photons) of order $\alpha^2(Z\alpha)^4 m$ to the energy levels. The vacuum polarization contribution is known to order e^4 from the work of Baranger, Dyson, and Salpeter (96). The fourth order self-energy corrections to the bound electron need only be calculated to lowest order in $F_{\mu\nu}$ and can be computed from the fourth order corrections to the form factors of the free electron vertex [Mills and Kroll (1954)]. Specifically, Lamb shift terms of order $(\frac{\alpha}{\pi})^2 (Z\alpha)^4 m$ are obtained from the fourth order anomalous moment and the slope of the Dirac form factor $F_1(q^2)$ at $q^2 = 0$. [See Equations 3.7 , 3.29.]

Recently the solution to a Lamb shift discrepancy of many years' standing has been resolved due to a new calculation of F_1' in fourth order. The new result, obtained by Appelquist and Brodsky (1970), is

$$m^2 \left. \frac{dF_1^{(4)}}{dq^2} \right|_{q^2=0} = [0.48 \pm 0.07] \left(\frac{\alpha}{\pi}\right)^2 \quad 3.28$$

and is obtained utilizing algebraic and numerical computer techniques similar to those used by Aldins et al. for $a_{\mu}^{\gamma\gamma}$. The error limits correspond to a 3σ confidence level for numerical evaluation of the required 5-dimensional parametric integrals. The new calculation differs from the previous result, $m^2 F_1' = 0.108 \left(\frac{\alpha}{\pi}\right)^2$, obtained analytically by Soto (99), [see also Weneser, Bersohn, and Kroll (100)], due to a discrepancy in overall sign and different numerical results for the non-infrared remainders of two of the five fourth-order Feynman graphs [the same graphs which give the

fourth order anomalous moment]. The revision accounts for an upward shift in the theoretical Lamb shift of 0.35 ± 0.07 MHz [$Z^4(2/n)^3$] and essentially reconciles theory and experiment, as discussed below. The crucial parts of the Appelquist-Brodsky results have now been confirmed by deRafael, Lautrup, and Petermann (101). It would be desirable, however, to eliminate the error limits introduced from numerical integration common to those recent calculations.

Relativistic recoil corrections.--Even without radiative corrections of the electron self-energy type, the spectrum of the hydrogenic atom which emerges from the Bethe-Salpeter equation is considerably more complicated than a reduced mass modification of the Dirac-Sommerfeld formula for an electron in a Coulomb field plus nuclear spin (hyperfine) interactions. The first rigorous treatment of the finite nuclear mass "recoil" corrections to the fine structure [of order $(Z\alpha)^5 m_e^2/M_N (e_1 \log Z\alpha + e_0)$] was given by Salpeter (79)]. Such terms arise from (a) that part of the two-Coulomb photon exchange not already contained in the iteration of the Coulomb potential of the Breit equation, (b) the exchange of two transverse photons (spin independent Thomson scattering on the nucleus), and (c) the retardation part of the transverse interaction due to one photon exchange.⁸ The latter contribution is similar to the non-relativistic approximation of the self-energy correction due to transverse photons (3.2) [multiplied by $2Z m_e/M_N$] and requires the retention of binding corrections in the energy denominator to avoid an infrared divergence. This is the source of

the $(Z\alpha)^5 m_e^2/M_N \log Z\alpha$ terms.

Grotch and Yennie (102) have recently given an alternate and somewhat simpler method for determining the finite proton mass corrections to the Dirac levels. An effective potential for the Dirac equation is derived which reproduces electron-proton scattering in one photon-exchange approximation. The resulting equations turn out to have the same eigensolutions as the usual Dirac equation but with modified parameters m' and α' . The resulting spectrum contains the correct m_e/M_N modifications of the fine structure levels. The $(Z\alpha)^5 m_e^2/M_N$ terms are then found from the effective potentials induced by contributions similar to (a), (b), (c) above. The results agree with those of Salpeter. The extension of the results to $n \neq 2$ has been given by Erickson (103).

The final nuclear correction which needs evaluation is the effect of nuclear size, specifically the modification of the Coulomb potential due to the change form factor of the proton. The result is by a simple and direct first order calculation (94)

$$\Delta E_{FS} = \delta \lambda_0 \frac{(Z\alpha)^4 m}{n^3} 4m^2 \frac{dG_E(q^2)}{dq^2} (q^2=0) \quad 3.29$$

This is 0.127 MHz for the $2S_{1/2}-2P_{1/2}$ separation in H using the Hand, Miller Wilson fit of the proton form factors. [Note that G_E automatically includes the spin-independent contribution of the F_2 form factor.] It is easy to check that nuclear polarization contributions are second order in m_e/M_p and are completely negligible for the Lamb shift (104).

Comparison with experiment.--A complete and compact formula for the $nS_{1/2}$ - $sP_{1/2}$ separation has been given by Taylor et al. (34, Equation 138a). [As we have discussed, the value of the fourth order slope of the electron F_1 form factor should be changed from $\frac{1}{2} m = 0.108$ to 0.48 ± 0.07 ; this leads to a correction of $+(0.35 \pm 0.07) Z^4 (2/n)^3$ MHz.] The breakdown for the various theoretical contributions to the $2S_{1/2}$ - $2P_{1/2}$ separation in H is given in Table 2 and the theoretical value of the various Lamb shift intervals of experimental interest are given in Table 3. In addition to the numerical uncertainty from the fourth order slope and the small uncertainties in the fundamental constants, the limits of error estimated by Erickson and Yennie (94) for uncalculated terms of order $\alpha(Z\alpha)^6 m$, $\alpha^2(Z\alpha)^5 m$ and $(Z\alpha)^5 m^2/M_N$ are used. The actual evaluation of these contributions will be an extremely arduous task. For example, evaluation of the order $\alpha^2(Z\alpha)^5 m$ contribution will require knowledge of the fourth order form factors for all q^2 plus evaluation of all fourth order improper graphs, e.g. cross terms between vacuum polarizations and self energy corrections.

The comparison of theory with experiment (see Table 3) now shows quite satisfactory agreement because of the recent modification of the theoretical result for dF_1/dq^2 in fourth order. This result is a landmark in removing the only major difficulty for QED at this time. The remaining inconsistencies appear more as contradictions between the various experiments than with theory. In the next section we will briefly review some of the theoretical questions involved in the analyses of the experimental results.

The fine structure separation.--We turn next to the full fine structure interval between the $2P_{3/2}$ and $2P_{1/2}$ states in hydrogen as illustrated in Figure 12. Since these p-states with $\ell \neq 0$ have vanishing wave functions at the origin, only a very few of the QED and relativistic recoil corrections discussed above affect the fine structure and their contributions are very small. Thus the exotic effects probed by the Lamb shift are generally absent since the electron and proton do not intrude into each other's private domains of "charge clouds". The theoretical prediction is given by a very simple formula

$$\Delta E(2P_{3/2}-2P_{1/2}) = \frac{Z^2 R_y \alpha (Z\alpha)^2 c}{16} \left[\left(1 + \frac{5}{8}(Z\alpha)^2\right) \left(1 - \frac{m_e}{M_p}\right) + 2a_e \left(1 - 2m_e/M_p\right) - \alpha/\pi (Z\alpha)^2 \log(Z\alpha)^{-2} \right] \quad 3.30$$

This is just the Dirac-Sommerfeld formula corrected for reduced mass effects (102) and the electron anomalous magnetic moment a_e . The last term is a radiative self-energy correction (94, 105) and only amounts to 1.2 ppm. The neglected terms are of order 0.3 ppm from neglected radiative corrections of relative order $\alpha(Z\alpha)^2$ and higher order recoil corrections. Using the Josephson junction value described earlier as the canonical one for α : $\alpha^{-1} = 137.03608(26)$, we can translate the above formula into a number for comparison with experiment (34)

$$\Delta E^{\text{th}}(2P_{3/2}-2P_{1/2}) = 10969.026 \pm 0.042 \text{ MHz } (1\sigma) \quad 3.31$$

On the other hand, because of its insensitivity to the exotic QED and Bethe-Salpeter equation effects, the precision determination can be used, as was done historically, to yield a very accurate number

for the fine structure constant. Now with the Josephson junction method we have two independent techniques to serve as mutual checks.

The fine structure separation has now been determined directly by the level crossing experiment of Metcalf, Baird, and Brandenberger (106). Their result (34)

$\Delta E^{\text{exp}} = 10969.127 \pm 0.095$ MHz (1 σ) and the inferred value for α : $\alpha^{-1} = 137.0354 \pm 0.0006$ are in quite satisfactory agreement with the non-QED determination. The various experimental determinations of the $2P_{3/2} - 2S_{1/2}$ separation in H and D can be combined with Lamb shift results to also obtain (somewhat variable) results for the fine structure separation (34). We have utilized the large interval measurements as further determinations of the shift of the $2S_{1/2}$ state, which is a more sensitive theoretical question [see Table 3].

The Lamb shift and fine structure experiments.--It would be difficult to overestimate the importance of the measurements of Lamb and his co-workers (107-109) on the development of QED. It is also remarkable that, despite the development of new techniques, subsequent measurements have shown no significant improvement in accuracy. We only wish to describe here the general schematic of the experiments and some of the theoretical questions which are involved. Extensive descriptions and analyses of errors, etc., may be found in the reviews by Taylor et al. (34), and Lea (110), and published lectures by Robiscoe (111) and Kleppner (112) in addition to the original articles.

In the experiments developed by Lamb and co-workers (107-109), a beam of atoms (H or D) was produced in the metastable $2S$ state ($\tau_{1/2} \sim 1/8$ sec) and passed through a microwave interaction and magnetic field region to a detector in which the metastable atoms ejected electrons from a metal surface. When the microwave frequency was adjusted to a $2S$ - $2P$ energy difference the transitions to the fast decaying $2P$ level diminished ("quenched") the intensity of the metastable beam at the detector. The magnetic field at which the transition occurs for a given microwave frequency, together with an extrapolation of the Zeeman levels from 1000 gauss to zero magnetic field, determines the $2S_{1/2}$ - $2P_{1/2}$ (or $2S_{1/2}$ - $2P_{3/2}$) energy separation of interest. Since individual hyperfine levels were not separated out, the resonance signal as a function of magnetic field is a double-humped curve with a width of about 100 MHz due mostly to the natural decay of the $2P$ level.

More recently, measurements of the Lamb shift in H and D have been made by Robiscoe (113) and Cosens (114) using a level crossing technique developed by Robiscoe and Lichten. No microwave field is needed since the $2S$ beam is quenched by a static electric field at a $2S$ - $2P$ crossing point of the magnetic level. An important advance in this work is that the metastable beam could be prepared in either of the two hyperfine levels. Thus the quenching signal was a single resonance curve and the asymmetry corrections were correspondingly small ($\sim 1/3$ MHz).

The $2S_{1/2}$ - $2P_{3/2}$ transition has recently been measured using a non-atomic beam "bottle method" technique of Kaufman et al. (115). The signal of a $2S_{1/2}$ - $2P_{3/2}$ microwave transition is the decay

radiation of the upper level. The direct measurement of the fine structure $2P_{3/2}-2P_{1/2}$ interval by Metcalf et al. (106) utilizes a resonance fluorescence technique. Photons which excite the $1S-2P$ transitions will scatter anomalously at 90° as the $2P_{1/2}$ and $2P_{3/2}$ levels become degenerate at a Zeeman crossing point. The Zeeman theory required for the extrapolation to zero field must be accurate to 1 ppm.

The two common features of these atomic fine structure measurements are thus photon-resonant scattering and a detailed calculation of the Zeeman structure. The Bethe-Lamb theory is utilized in these experiments to understand the observed resonance signal and locate its line center to an accuracy of 0.1 MHz. (In the Lamb experiments this is one-thousandth of the line width!) Various asymmetry and shift corrections (up to 1 MHz) have to be included for matrix element variation, Zeeman curvature, quenching asymmetries, and the Stark effect. There has been some basic theoretical work on the validity of such analyses. Low (25) has analyzed resonant scattering on the atom and determined that the radiative corrections and anti-resonant signals will skew the theoretical curve at relative order α^3 . A theoretical analysis (116) of the electromagnetic current of the relativistic atom has established that the usual Breit (one-time) external interaction Hamiltonian, which is used as the basis of the calculations of the Zeeman levels, is correct at least through order $(Z\alpha)^2 m_e/M_N$ (Brodsky and Primack, 1969). The spectrum of the resulting Zeeman Hamiltonian can be explicitly solved to better

than 1 ppm accuracy (117, 118).

The results of the various experiments are given in Table 3. The assigned errors are those given in ref. 34 and represent a one standard deviation confidence level including statistical and systematic errors. The results shown for Robiscoe's and Cosens' measurements of the Lamb intervals in H and D have revised velocity-dependent asymmetry corrections calculated from the Robiscoe-Shyn (113) determination of the atomic beam velocity distribution.

The hyperfine splitting in H and μ^+e^- . --The hyperfine splitting (hfs) in atomic hydrogen, i.e. the energy shift due to the interaction of the electron with the proton's magnetic moment is an important historic link between the usually disconnected fields of high energy and precision atomic physics. This is because the basic Fermi interactions for S-states is of short range $\sim \vec{\mu}_e \cdot \vec{\mu}_p \delta^3(r)$ and its modifications are sensitive to details of proton structure which are usually seen only in high-energy electron-proton elastic and inelastic scattering experiments. At this time, given our total success with QED in its many precise applications, the main significance of hfs measurements are to probe the proton's structure, although its historic role was to probe QED to the limits set by the proton's unknown behavior.

The theoretical splitting between the triplet and singlet states of the ground state of H is (119)

$$\begin{aligned}
\nu_{\text{hfs}} = & \frac{16}{3} \text{Ry}_{\infty} \alpha^2 c \frac{\mu_{\text{N}}}{\mu_{\text{B}}} \left(1 + \frac{m_{\text{e}}}{M_{\text{N}}}\right)^{-3} \\
& \left\{ 1 + a_{\text{e}} + \frac{3}{2} (Z\alpha)^2 + \alpha(Z\alpha) \left(-\frac{5}{2} + \log 2\right) \right. \\
& + \frac{\alpha}{\pi} (Z\alpha)^2 \left[-\frac{2}{3} \log^2(Z\alpha)^{-2} + \left(\frac{37}{72} + \frac{4}{15} - \frac{8}{3} \log 2\right) \log(Z\alpha)^{-2} + 18.36\pm 5 \right] \\
& \left. + \delta_{\text{N}} + \delta_{\text{N}}^{\text{pol}} \right\} \quad 3.32
\end{aligned}$$

which takes the form of the Fermi frequency due to a point magnetic dipole in the proton interacting at zero range with the electron moment in a spherical S-state, modified by corrections due to the electron anomalous moment, v^2/c^2 binding corrections from the Dirac equation, radiative corrections of order α (from the self-energy correction--Eq. 3.27--expanded to first order in the hfs potential, plus vacuum polarization corrections), and nuclear size and polarizability corrections. The order $\alpha(Z\alpha)$ term was first calculated by Kroll and Pollack (120) and Karplus, Klein and Schwinger (121); the $\log(Z\alpha)$ terms were calculated by Layzer (122) and Zwanziger (123). A comprehensive recalculation of these radiative corrections plus the dominant contribution to the $\alpha(Z\alpha)^2$ non-log term and an estimate of uncalculated radiative terms has been given by Brodsky and Erickson (119). The dominant nuclear size correction from the static magnetic moment and charge distribution was first obtained by Zemach (124) for $M_{\text{N}} \rightarrow \infty$ as a term $\delta_{\text{N}}(\text{size}) = -2 Z\alpha m R_{\text{pr}} = -38.2$ ppm where R_{pr} is an appropriate nuclear radius obtained from a convolution of the G_{E} and G_{M} form factors obtained from elastic e-p scattering.

The complete covariant treatment of the nuclear finite size and finite mass (recoil) corrections of the proton, [treating the proton as an extended (but rigid) distribution] leads to additional corrections of relative order $Z\alpha m_e/M_p$. The numerical result of Iddings and Platzman, and confirmed by Grotch and Yennie (102) [see also Guerin (126), Iddings (127), Faustov (128), Cherniak, Faustov, Zinovjev (129)] adds +3.6 ppm leaving a total contribution from a rigid non-polarizable proton of $\delta_N = -34.6 \pm 0.9$ ppm (allowing for uncertainties in the form factors). [For a complete review of these corrections see Grotch and Yennie (102).]

The contribution of nuclear polarization to the hfs of H [see Figure 13e] is an extremely important subject since its calculation involves, in principle, most of the uncertainties of proton dynamics. For the hfs we are interested in spin-dependent dynamical quantities (whose spin-independent but isotopic-dependent parts are required for the calculations of the n-p mass difference, a program of limited success thus far). These current matrix elements also enter the study of inelastic e-p scattering which is currently of great interest and under intense study. The key in all of this work is Cottingham's (130) observation that the closed loop integrals in Figure 13e can be rewritten by rotating the contour of the photon momentum integral to extend only over spacelike photons. This is the region accessible to dispersion analyses in terms of inelastic scattering amplitudes. However the hfs contribution from inelastic states has a more convergent mass-

difference calculation (because of the additional electron propagator), and it is found (126,127,131) that single N^* excitation channels contribute less than 1 ppm if smooth behavior of the electro-production amplitudes for very virtual photons is assumed. In principle, the complete result for proton excitation may be obtained from an integration over the inelastic form factors obtained from spin-dependent inelastic e-p scattering (129). Such data may eventually rule out large polarization contributions of order 5-10 ppm which can be obtained readily from conventional but non-relativistic composite models of the proton (132). Bjorken (133) has estimated that current algebra (a model that would give point-like constituent structure for the hadronic interactions of very virtual photons) leads to small ($\lesssim 3$ ppm) polarization corrections. There are also additional corrections possible from the direct transverse coupling of an electron via two photons to the proton through an axial vector meson (the A_1), but this is probably negligible from the experimental equality of e^+p and e^-p scattering at high momentum transfer (134).

The physical idea behind the polarizability contribution is this. To the extent that the proton is polarizable, the circulating electron can adjust its orbit to follow the instantaneous charge distribution of the proton rather than its spherical average as described for a rigid structure by the elastic form factors. Such an adjustment would cancel a considerable portion of the finite size correction of -35 ppm described above. This is the case as observed for the deuterium hfs where the loosely-bound deuterium

is highly polarizable, as was first shown by A. Bohr (135). The proton is much less polarizable than the deuteron, its excited states lying at least 140 MeV above its ground state. However, it would be our conclusion that once one is working at an accuracy of 10 ppm, it is nuclear dynamics, not QED, that is being probed.

There is no question about the reliability of the experimental result. The most recent measurement by Vessot et al. (136) is an unbelievably precise value

$$\nu_H^{\text{exp}} = 1420.405\,751\,7864(17) \text{ MHz } (\pm 1.2/10^{12}) \quad 3.33$$

using the hydrogen maser technique of Crampton, Kleppner, and Ramsey (137). Using $\alpha^{-1} = 137.03608(26)$, and leaving the proton polarizability contribution as a parameter, one finds

$$\frac{\nu_H^{\text{exp}} - \nu_H^{\text{th}}}{\nu_H^{\text{exp}}} = 2.5 \pm 4.0 \text{ ppm} - \delta_N^{\text{pol}} \quad 3.34$$

which is consistent with a small polarization correction.⁹ Note that experiment has been moved seven orders of magnitude beyond theoretical challenge.

The hadron dynamics problem is avoided by studying the hyperfine splitting of the ground state of muonium (μ^+e^-) measured in pioneering experiments by Hughes and co-workers (140). The dynamics of this atom is completely specified by QED and the Bethe-Salpeter equation. The hfs of the ground state is still given by (3.32) but the nuclear correction is removed and replaced by known electrodynamic contribution for a Dirac muon (141,142):

$$\delta_{\mu} = -\frac{3\alpha}{\pi} \frac{m_e}{m_{\mu}} \log \frac{m_{\mu}}{m_e} = -179.7 \text{ ppm.} \quad 3.35$$

We can interpret the muonium hfs either as an independent measure of the fine structure constant for comparison with the Josephson junction results or as a further probe of muon-electron universality.

The most recent measurement of the Yale group (143) is

$$v_{(\mu e)}^{\text{exp}} = 4463.249 \pm 0.031 \text{ MHz.} \quad 3.36$$

This result has been obtained through observations of hfs transitions in a very weak magnetic field and improves the precision beyond earlier results in both strong and weak fields. It also involves measurements over a wide range of gas pressures permitting an assumed linear extrapolation of the pressure shift of the splitting from the conditions where the experiments were conducted to zero.

A new result on the hfs has been reported by V. L. Telegdi and co-workers at the University of Chicago (144). Their method is a variant of the Yale experiment but is carried out at lower gas pressures in order to reduce uncertainty from extrapolation. The Chicago group accomplishes this by choosing the external Zeeman field B such that the microwave frequency is to first order field-independent. Their observation that such a choice exists enables them to work with a sample of larger volume without being very sensitive to inhomogeneities in B . Their result is:

$$v_{(\mu e)}^{\text{exp}} = 4463.317 \pm 0.021 \text{ MHz} \quad 3.37$$

which is within 2σ of the Yale result.

The main trouble with comparing theory with this experimental result is that the muon moment in Bohr magnetons or, alternatively, the electron/muon mass ratio is not known to sufficient precision. We can use the ratio of muon to proton magnetic moments as

measured in water if we correct the experimental result by the Ruderman (1966) estimate of the effect of diamagnetic shielding on the muon moment. This correction takes into account the fact that because of its lighter mass and resulting higher zero point energy, the μ^+ tends to sit in intermolecular space with less shielding of the applied field than the (H_2O -bound) protons.

Ruderman estimated a diamagnetic shielding of the muon moment of $\mu_\mu = \mu'_\mu(1 + \sigma_\mu)$, $\sigma_\mu \cong 10$ ppm which is small compared to the usual 26 ppm correction for the proton. Then, using the canonical value, $\alpha^{-1} = 137.03608(26)$, we find

$$v_{\mu e}^{th} = 4463.272 \pm 0.061 \text{ MHz} \quad 3.38$$

which beautifully overlaps both experiments. Further development of the theoretical treatment of the Ruderman effect, or a direct measurement of the muon moment using the double resonance method¹¹ discussed by Telegdi (146) will make the muonium hfs a key experiment in testing QED and the identification of the muon as "just a heavy electron".

Other hydrogenic systems.--Critical tests of QED are also possible in other bound systems:

(1) Lamb shift measurements in high Z-ions will probably be possible using beam foil techniques to strip the atom down to one electron (147). As has been discussed by Erickson (103) the Lamb shift in atomic mercury, measured via its ionization edge, is in disagreement with the theory of Brown and Mayers, although it is in agreement with recent calculations (within 5% accuracy) performed by Desiderio and Johnson.

(2) The fine structure of atomic helium can probably be determined to better than 1 ppm. The progress toward a theoretical calculation to this precision has been recently discussed by C. Schwartz (148) and L. Hambro (149).

(3) Positronium (e^+e^-) is the fundamental system for testing QED and the Bethe-Salpeter formalism. The most recent measurements (150) for the hfs of the ground state give $\nu_{e^+e^-}^{\text{exp}} = 203.403(12)$ GHz (± 50 ppm). The 3S_1 state lies above the 3S_0 level in part due to the dipole-dipole interaction as in the hydrogen hfs and in part due to the virtual annihilation of the e^+e^- pair in the triplet state into a single quantum.

The theoretical prediction is (151-153)

$$\begin{aligned} \nu_{e^+e^-}^{\text{th}} &= \alpha^2 \text{Ry}_{\infty} \left[\frac{7}{6} - \left(\frac{16}{9} + \ln 2 \right) \frac{\alpha}{\pi} + \alpha^2 \ln \alpha^{-1} + o(\alpha^2) \right] \\ &= 203.427(9) \end{aligned} \quad 3.39$$

where we have included the new results of order $\alpha^6 (\log \alpha)_m$ obtained recently in a remarkable calculation by Fulton, Owen, and Repko (153). The error limit used here is obtained from a simple estimate (153) of the expected size of the α^6_m term. Hopefully, there will be further work on the magnitude of this term as well as new measurements, which will enable the positronium hfs to become one of the crucial tests of fundamental theory.

(4) Muonic x-rays from $\mu^- \text{Bi}$ and $\mu^- \text{Pb}$ and other high Z muonic atoms have now been measured to better than 100 ppm. Compared with sensitive electron scattering measurements of the nuclear charge distribution, the muonic energy levels have confirmed the vacuum polarization corrections (due to electron loops) to a few

percent precision (154,155). Lamb shift effects due to the muon self-energy are now on the threshold of being seen (156).

(5) Although the experimental difficulties seem very formidable, a measurement of the Lamb shift or hfs of muonic hydrogen (μ -p) would be extremely interesting since the characteristic momentum transfers are 200 times larger than that of ordinary hydrogen. A novel aspect of this unique system, discussed in detail by Di Giacomo (157) is the odd arrangement of the 2S and 2P levels. Because of the huge effect of electron pair vacuum polarization, the $2S_{1/2}$ level lies well below the $2P_{1/2}$ level; the $2P_{1/2}-2S_{1/2}$ separation is 25 times larger than the fine structure interval. the self-energy shift is only a minor perturbation to the Lamb interval; the proton finite size corrections are in fact five times larger than those due to the self-radiative corrections to the muon.

The hyperfine separations in muonic hydrogen scale overall as the lepton mass squared, with reduced mass corrections and other contributions given as in 3.32 plus electron-pair vacuum

polarization corrections given by the work of Sternheim (139) and Di Giacomo (157). Relative to ordinary hydrogen the μ -p hfs has an extra power of m_μ/m_e in sensitivity to linear finite nuclear size and polarization corrections. A study of the fine and hyperfine structure of this fascinating and fundamental system can thus probe QED and proton structure at very short distances.

(6) Very precise measurements of the ratio of atomic g_J factors of ground state hydrogen and deuterium can be performed (see Hughes et al., 158 ; D. J. Larson et al., 159) which are sensitive to theoretical terms of order $(Z\alpha)^2 m_e/m_p$. The theoretical calculations and comparisons with experiment have been summarized by H. Grotch (1969). Measurements of the g_J ratio of H and He^+ would be sensitive to radiative corrections of relative order $\alpha(Z\alpha)^2$. Verification of such terms would be complementary to the other tests of QED in hydrogenic atoms.

4. CONCLUSIONS

Limits of the theory.--Quantum electrodynamics has never been more successful in its confrontation with experiment than it is now. There is really no outstanding discrepancy despite the fact that we are pursuing the limits of the theory to higher accuracy and smaller distances than what was possible even a few years ago. The progress is due to new experiments at high energy and high momentum transfer, especially those involving colliding e^+e^- beams; new precision measurements in hydrogenic atoms and anomalous moments of the muon and electron; the independent determination of α from the e/h Josephson junction measurements; and new algebraic and computational techniques which have considerably extended our calculational abilities, especially for the fourth order Lamb shift and sixth order anomalous moment results.

Breakdown of the theory of course could still occur at short distances or at higher precision if any of the following existed: a) intrinsic lepton size (non-local) currents or intrinsic anomalous moment; b) excited leptons (25); c) non-electromagnetic couplings of the leptons (77,161); d) heavy photons of positive or negative metric (4); e) existence of magnetic charge; f) breakdown of perturbation theory or anomalous subtraction constants not given by the renormalization procedure. All of these modifications are ruled out to some extent by the various tests as we have discussed above. In addition, the basic symmetry properties of QED, conservation laws, and secular constancy of α , c , etc. have all been checked to various degrees (162).

All of the suggested modifications would mar the essential simplicity of Maxwell's equation and the Dirac form of the lepton current. Despite this simplicity, however, and despite its phenomenal success, the fundamental problems of renormalization in local field theory and the nature of the exact solutions of quantum electrodynamics are still to be resolved.

Acknowledgements

We wish to thank Professors D. R. Yennie and G. W. Erickson and our colleagues at SLAC for their helpful suggestions.

LITERATURE CITED

1. The historical development of QED can be traced through the literature collection edited by J. Schwinger, 1958 Quantum Electrodynamics, New York: Dover Publications, Inc., 424 pp.
2. Goldhaber, A. S., Nieto, M. M., *Phys. Rev. Letters* 21, 567 (1968).
3. Barber, W. C., Gittelman, B., O'Neill, G. K., Richter, B., *Phys. Rev.* 16, 1127 (1966) and Proc. of 14th Int. Conf. on High Energy Physics, Vienna (1968).
4. Lee, T. D., Wick, G. C., *Nuclear Phys.* 39, 209 (1969).
Lee, T. D., talk given at Topical Conf. on Weak Interactions, CERN (1969).
5. Augustin, J. E., Buon, J., Belcourt, B., Haissinski, J., Jeanjean, J., et al., Proc. 1969 Intern. Symp. on Electron and Photon Interactions, Daresbury (1969).
6. Sidorov, V., Communications in the Proc. 1969 Intern. Symp. on Electron and Photon Interactions, Daresbury (1969).
7. McClure, J. A., Drell, S. D., *Nuovo Cimento* 37, 1638 (1965).
8. Kroll, N. M., *Nuovo Cimento* 45A, 65 (1966).
9. Gatto, R., in High Energy Physics, Edited by E. H. S. Burhop, N.Y.: Academic Press (1968), vol. II. (Rev. of QED up to 1968). We refer to this excellent and comprehensive review for a more detailed discussion and complete bibliography of these studies.
10. Tennenbaum, J., Eisner, A., Feldman, G., Lockeretz, W., Pipkin, F. M., Randolph, J. K., Proc. Intern. Symp. on Electron and Photon Interactions, Daresbury (1969).
11. Randolph, J. K., Eisner, A., Feldman, G., Lockeretz, W., Pipkin, F. M., Tennenbaum, J., Proc. Intern. Symp. on Electron and Photon Interactions, Daresbury (1969).
12. Biggs, P. J., Braben, D. W., Clifft, R., Gabathuler, E., Kitching, P., Rand, R. E., Proc. Intern. Symp. on Electron and Photon Interactions, Daresbury (1969).
13. Knasel, T. M. in Lectures in Theoretical Physics, 108, N.Y.: Gordon and Breach (1968), p. 549.
14. Brodsky, S. J., Invited talk, Proc. Intern. Symp. on Electron and Photon Interactions, Daresbury (1969).

15. Earles, D., von Briesen Jr., H., Chase, R., Faissler, W. et al., Proc. Intern. Symp. on Electron and Photon Interactions, Daresbury (1969).
16. Russell, J. J., Sah, R. C., Tannenbaum, M. J., Cleland, W. E., Ryan, D. G., Stairs, D. G., Proc. Intern. Symp. on Electron and Photon Interactions, Daresbury (1969).
17. Ellsworth, R. W., Mellissinos, A. C., Tinlot, J. H., von Briesen Jr., H., Yamanochi, T., et al., Phys. Rev. 165, 1449 (1968). See also Lederman, L. M., quoted by Panofsky, W. K. H., Proc. of 14th Int. Conf. on High Energy Physics, Vienna (1968), p. 23.
18. Greehut, G. K., Weinstein, R., Parsons, R. G., University of Texas preprint, report no. CPT-17 (1969).
19. Asbury, J. G., Becker, U., Bertram, W. K., Joos, P., Rohde, M. et al., Phys. Rev. Letters 19, 869 (1967); Alvensleben, H., Becker, U., Bertram, W. K., Binkley, M., Cohen, K. et al., Phys. Rev. Letters 21, 1501 (1968).
20. Augustin, J. E., Bizot, J. C., Buon, J., Haissinski, J., Lalanne, D. et al., Physics Letters 28B, 503, 508, 513 (1969). See also Perez-Y-Jorba, J., Invited talk Proc. Intern. Symp. on Electron and Photon Interactions, Daresbury (1969).
21. Auslander, V. L., Budker, G. I., Pakhtusova, E. V., Pestov, Yu. N., Sidorov, V. A. et al., Yadernaya Fizika 9 114 (1969).
22. Hayes, S., Imlay, R., Joseph, P. M., Keizer, A. S., Knowles, J. et al., Cornell University, preliminary report.
23. Becker, U., Bertram, W. K., Binkley, M., Jordan, C. L., Knasel, T. M. et al., Phys. Rev. Letters 21, 1504 (1968).
24. Augustin, J. E., Bizot, J. C., Buon, J., Haissinski, J., Lalanne, D. et al., Physics Letters 28B, 517 (1969).
25. Low, F., Phys. Rev. Letters 14, 238 (1968).
26. Gutbrod, F., Schildknecht, D., Zeit, F., Physik 192, 271 (1966).
27. Budnitz, R., Dunning, J. R., Gotein, M., Ramsey, N. F., Walker, J. Wilson, R., Phys. Rev. 141, 1313 (1966).
28. Behrend, H. J., Brasse, F. W., Engler, J., Ganssaue, E., Hultschig, S., et al., Phys. Rev. Letters 15, 900 (1965).

29. Betourne, C., Nguyen Ngoc, H., Perez-y-Jorba, J.,
Tran Thanh Van, J., Phys. Letters 17, 70 (1965).
30. Boley, C. D., Elias, J. E., Friedman, J. I., Hartman, G. C.,
et al., Phys. Rev. 167, 1275 (1968).
31. Parker, S., Anderson, H. L., Rey, C., Phys. Rev. 133B,
768 (1964).
32. Frankel, S., Fraiti, W., Halpern, J., Nuovo Cimento 27,
894 (1963).
33. Barber, W. C., Gittelman, B., O'Neill, G. K., Richter, B.,
Phys. Rev. Letters 22, 902 (1969).
34. Taylor, B. N., Parker, W. H., Langenberg, D. N., Rev.
Mod. Phys. 41 (1969).
35. Parker, W. H., Taylor, B. N., Langenberg, D. N., Phys.
Rev. Letters 18, 287 (1967).
36. Finnegan, T. F., Denenstein, A., Langenberg, D. N., Phys.
Rev. Letters 24, 738 (1970).
37. Clarke, J., Phys. Rev. Letters 21, 1566 (1968).
38. Feynman, R. P., Leighton, R. B., Sands, M., The Feynman
Lectures on Physics, Reading: Addison-Wesley (1963),
Vol. 3.
39. Nordtvedt, K., Phys. Rev. (to be published).
40. Wilkinson, D. T., Crane, H. R., Phys. Rev. 130, 852 (1963).
41. Rich, A., Phys. Rev. Letters 20, 967, 1221 (1968).
42. Henry, G. R., Silver, J. F., Phys. Rev. 180, 1262 (1969).
43. Gilleland, J., Rich, A., Phys. Rev. Letters 23, 1130 (1969).
44. Rich, A. (private communication).
45. Gräff, G., Major, F. G., Roeder, R. W. H., Werth, G., Phys.
Rev. Letters 21, 340 (1968).
46. Dehmelt, A. (unpublished).
47. See, e. g. Bjorken, J. D., Drell, S. D., Relativistic
Quantum Fields, N.Y.: McGraw-Hill (1964).
48. Appelquist, T., Primack, J., (to be published).

49. Schwinger, J., Phys. Rev. 73, 416 (1948), 76, 790 (1949).
50. Karplus, R., Kroll, N. M., Phys. Rev. 77, 536 (1950).
51. Sommerfield, C. M., Phys. Rev. 107, 328 (1957); Ann. Phys. (N.Y.) 5, 26 (1958).
52. Petermann, Helv. Phys. Acta 30, 407 (1957).
53. Terentev, M. V., Zh. Eksp. i Teor. Fiz 43, 619 (1962)
[Translation: Sov. Phys.-JETP 16, 444 (1963)]
54. Drell, S. D., Pagels, H. R., Phys. Rev. 140, B397 (1965).
55. Parsons, R. G., Phys. Rev. 168, 1562 (1968).
56. Mignaco, J. A., Remiddi, E., Nuovo Cimento 60A, 519 (1969).
57. Aldins, J., Kinoshita, T., Brodsky, S. J., Dufner, A.,
Phys. Rev. Letters 23, 441 (1969), and Phys. Rev.
(to be published).
58. Hearn, A. C., Stanford University Report ITP-247 (1969).
59. Bailey, J., Bartl, W., von Bochman, G., Brown, R. C. A.,
Farley, F. J. M., Jöstlein, H., Picasso, E., Williams,
R. W., Phys. Letters 28B, 287 (1968).
60. Farley, F. J. M., Invited Paper at the First Meeting of
the European Physical Society at Florence (1969).
61. Elend, H. H., Phys. Letters 20, 682, 21, 720 (1966).
See also Erickson, G. W., and Liu, H. (unpublished).
62. Suura, H. and Wichmann, E. H., Phys. Rev. 105, 1930 (1957).
63. Petermann, A., Phys. Rev. 105, 1931 (1957), Fortschr.
Physik 6, 505 (1958).
64. Drell, S. D., Trefil, J. (unpublished), See Drell, S. D.,
Proc. of the 13th International Conference on High
Energy Physics (Berkeley, 1966) p. 93 and Drell, S. D.,
in Particle Interactions at High Energies, Scottish
University Summer School, Ed. by T. W. Priest and L. L. J.
Vick, Edinburgh: Oliver and Boyd (1966).
65. Kinoshita, T. K., Nuovo Cimento 51B, 140 (1967) and
Cargese Lectures in Physics, Vol. 2 (Gordon and Breach,
New York, 1968) p. 209.
66. Lautrup, B. and de Rafael, E., Phys. Rev. 174, 1835 (1968).

67. The results of the Orsay experiments are given in ref. 20.
68. Gourdin, M., de Rafael, E., Nuclear Phys. 10B, 667 (1969).
69. Terazawa, H., Progr. Theoret. Phys. (Kyoto) 39, 1326 (1968).
70. Etim, E., and Picchi, P., Frascati preprint LNF-69133 (1969).
71. Bell, J., de Rafael, E., CERN preprint TH-1019 (1969).
72. Brodsky, S. J., Sullivan, J. D., Phys. Rev. 156, 1644 (1967).
73. Burnett, T., Levine, M. J., Phys. Letters 24B, 467 (1967).
74. Shaffer, R. A., Phys. Rev. 135, B187 (1967).
75. Lee, T. D., Phys. Rev. 128, 899 (1962).
76. Gell-Mann, M., Goldberger, M. L., Kroll, N. M., Low, F. E., Phys. Rev. 179, 1518 (1969). See also Rai Choudhury, S.,
77. Brodsky, S. J., de Rafael, E., Phys. Rev. 168, 1620 (1965).
78. Bailey, J., Picasso, E., (to be published in Nucl. Physics).
79. Salpeter, E. E., Bethe, H. A., Phys. Rev. 84, 1232 (1951);
Salpeter, E. E., Phys. Rev. 87, 328 (1952).
80. Gell-Mann, M., Low, F., Phys. Rev. 84, 350 (1951).
81. Mandelstam, S., Proc. Roy. Soc. (London) A238, 248 (1955).
82. Low, F., Phys. Rev. 88, 53 (1952).
83. Yennie, D. R. (private communication).
84. Brown, L. S. (private communication).
85. Brodsky, S. J., Brandeis Lectures in Theoretical Physics 1969
N.Y.: Gordon and Breach (to be published).
86. Bethe, H. A., Phys. Rev. 72, 339 (1947).
87. Welton, T. A., Phys. Rev. 74, 1157 (1948), see discussion
in ref. 47.
88. Bethe, H. A., Brown, L. M., Stehn, J. R., Phys. Rev. 77,
370 (1950).
89. Schwartz, C., Tiemann, J. J., Ann. Phys. (N.Y.) 6, 178 (1959).
90. Harriman, J. M., Phys. Rev. 101, 594 (1956).

91. Huff, R. W., Phys. Rev. 186, 1367 (1969).
92. Serber, R., Phys. Rev. 48, 49 (1935).
93. Uehling, E. A., Phys. Rev. 48, 55 (1935).
94. Erickson, G. W., Yennie, D. R., Ann. Phys. (N.Y.) 35, 271, 447 (1965).
95. Fried, H. M., Yennie, D. R., Phys. Rev. Letters 4, 583 (1960).
96. Baranger, M., Dyson, F., Salpeter, E., Phys. Rev. 88, 680 (1952).
97. Mills, R. L., Kroll, N. M., Phys. Rev. 98, 1489 (1955).
98. Appelquist, T., Brodsky, S. J., Phys. Rev. Letters 24, 562 (1970).
99. Soto, Jr., M. F., Phys. Rev. Letters 17, 1153 (1966).
100. Weneser, J., Bersohn, R., Kroll, N. M., Phys. Rev. 91, 1257 (1953).
101. de Rafael, E., Lautrup, B., Petermann, A., CERN preprint TH-1140, 1970 (to be published).
102. Grotch, H. and Yennie, D. R., Rev. Mod. Phys. 41, 350 (1969).
103. Erickson, G. W., Physics of One-and Two-Electron Atoms, F. Bopp and H. Kleinpoppen, Eds. Amsterdam: North Holland Publishing Company (1969).
104. Petrunkin, V. A., Semenko, S. F., Yadernaya Fizika 3, 489 (1966).
105. Layzer, A. J., Phys. Rev. Letters 4, 580 (1960).
106. Metcalf, H., Brandenberger, J. R., Baird, J. C., Phys. Rev. Letters 21, 165 (1968).
107. Lamb, Jr., W. E., Phys. Rev. 85, 259 (1952).
108. Lamb, Jr., W. E., Retherford, R. C., Phys. Rev. 79, 549 (1950), 81, 222 (1951), 86, 1014 (1952).
109. Triebwasser, S., Dayhoff, E. S., Lamb, Jr., W. E., Phys. Rev. 89, 98 (1953).
110. Lea, K. R., Invited talk, A.P.S. Meeting (1968).

111. Robiscoe, R., in Lectures in Theoretical Physics, N.Y.: Gordon and Breach, 1970 (to be published).
112. Kleppner, D., Brandeis Lectures in Theoretical Physics, N.Y.: Gordon and Breach, 1969 (to be published).
113. Robiscoe, R. T., Shyn, T. W., Phys. Rev. Letters 24, 559 (1970); Robiscoe, R., Phys. Rev. 168, 4 (1968).
114. Cosens, B. L., Phys. Rev. 173, 49 (1968).
115. Kaufman, S. L., Lamb, Jr., W. E., Lea, K. R., Leventhal, M., Phys. Rev. Letters 22, 507 (1969).
116. Brodsky, S. J., Primack, J. R., Ann. Phys. 52, 315 (1969), Phys. Rev. 174, 2071 (1968).
117. Brodsky, S. J., Parsons, R. G., Phys. Rev. 163, 134, 176, 423 (1967).
118. Kaufman, S. L. (private communication).
119. Brodsky, S. J. and Erickson, G. W., Phys. Rev. 146, 26 (1966) and refs. therein.
120. Kroll, N. M., Pollack, F., Phys. Rev. 84, 594, 86, 876 (1951).
121. Karplus, R., Klein, A., Schwinger, J., Phys. Rev. 84, 597 (1951).
122. Layzer, A. J., Phys. Rev. Letters 4, 580; J. Math. Phys. 2, 292, 308 (1961); Nuovo Cimento 33, 1538 (1964).
123. Zwanziger, D., Nuovo Cimento 34, 77 (1964).
124. Zemach, C., Phys. Rev. 104, 1771 (1956).
125. Iddings, C. K., Platzman, P. M., Phys. Rev. 113, 192, 115, 919 (1959).
126. Guerin, F., Nuovo Cimento 50A, 1, 211 (1967).
127. Iddings, C. K., Phys. Rev. 138, B446 (1969).
128. Faustov, R. N., Nucl. Phys. 75, 669 (1966).
129. Cherniak, V. L., Faustov, R. N., Zinojev, G. M., Struminski, B. V., Dubna preprints (1969).
130. Cottingham, W. N., Ann. Phys. (N.Y.) 25, 424 (1963).

131. Verganalakis, A., Zwanziger, D., Nuovo Cimento 39, 613 (1965).
132. Drell, S. D., Sullivan, J. D., Phys. Rev. 154, 1477 (1967).
133. Bjorken, J. D., Phys. Rev. 148, 1467 (1966).
134. Drell, S. D., Sullivan, J. D., Phys. Letters 19, 516 (1966).
135. Bohr, A., Phys. Rev. 73, 1109 (1948); see also F. Low, Phys. Rev. 77, 361 (1950).
136. Vessot, R., et al., IEEE Trans. Instr. Meas. IM-15, 165 (1966).
137. Crampton, S. B., Kleppner, D., Ramsey, N. F., Phys. Rev. Letters 11, 338 (1963).
138. Fortson, E. N., Major, F. G., Dehmelt, H. G., Phys. Rev. Letters 16, 221 (1966).
139. Sternheim, M., Phys. Rev. 130, 211 (1963).
140. Hughes, V., Phys. Today 20, 29 (December, 1967), Proc. of the First Intern. Conf. on Atomic Physics (Plenum Press, Inc., New York, 1969).
141. Newcomb, W. A., Salpeter, E. E., Phys. Rev. 97, 1146 (1955).
142. Arnowitt, R., Phys. Rev. 92, 1002 (1953).
143. Crane, P., Amato, J. J., Hughes, V. W., Lazarus, D. M., zu Putlitz, G., Thompson, P. A., Proc. Intern. Symp. on Electron and Photon Interactions, Daresbury (1969).
144. Ehrlich, R. D., Hofer, H., Magnon, A., Stowell, D., Swanson, R. A., Telegdi, V. L., Chicago University Preprint EFINS-69-71 (1969).
145. Ruderman, M. A., Phys. Rev. Letters 17, 794 (1966).
146. Telegdi, V., (private communication).
147. Bashkin, S., Phys. Rev. 162, 12 (1967).
148. Schwartz, C., Proc. of the First Intern. Conf. on Atomic Physics, N.Y.: Plenum Press, Inc., (1969).
149. Hambro, L., Ph.D. Thesis, Univ. of California, 1970, (unpublished).

150. Theriot, Jr., E. D., Beers, R. H., Hughes, V. W., Phys. Rev. Letters 18, 767 (1967).
151. Karplus, R., Klein, A., Phys. Rev. 87, 848 (1952).
152. Erickson, G. W. (unpublished), quoted in ref. 34.
153. Fulton, T., Owen, D., Repko, W. W., Johns Hopkins University preprint, 1970.
154. Telegdi, V., Proc. of the First Intern. Conf. on Atomic Physics (Plenum Press, Inc., New York, 1969).
155. Anderson, H. L., Hargrove, K., Hincks, E. P., McAndrew, J. D., McKee, R. J., et al., Phys. Rev. Letters 22, 221 (1969).
156. Barrett, R. C., Brodsky, S. J., Erickson, G. W., Goldhaber, M. H., Phys. Rev. 166, 1589 (1968).
157. Di Giacomo, A., Nucl. Phys. B11, 411 (1969).
158. Hughes, W. M., Robinson, H. G., Phys. Rev. Letters 23, 1209 (1969).
159. Larson, D. J., Valberg, P. A., Ramsey, N. F., Phys. Rev. 184, 14 (1969).
160. Grotch, H., Phys. Rev. Letters 24, 39 (1970).
161. Lee, T. D., Zumino, B., Phys. Rev. 163, 1667 (1967).
162. For a review see Feinberg, G., Proc. of the First Intern. Conf. on Atomic Physics, (Plenum Press, Inc., New York, 1969).
163. Cohen, K. J., Homma, S., Luckey, D., Osborne, L. S., Phys. Rev. 173, 1339 (1968).
164. Eisenhandler, E., Feigenbaum, J., Mistry, N., Mostek, P., Rust, D., et al., Phys. Rev. Letters 18, 425 (1967).
165. de Pagler, J. K., Friedman, J. I., Glass, G., Chase, R. C., Gettner, M., et al., Phys. Rev. Letters 17, 767 (1967).
166. Quinn, D. J., Ph.D. Thesis, Stanford University, Stanford, California (unpublished, 1968).

167. Siemann, R. H., Ash, W. W., Berkelman, K., Hartill, D. L., Lichtenstein, C. A., Littauer, R. M., Phys. Rev. Letters 22, 421 (1969).
168. Liberman, A. D., Hoffman, C. M., Engels, E., Jr., Imrie, D. C., Innocenti, P. G., et al., Proceedings Intern. Symp. on Electron and Photon Interactions, Daresbury (1969).
169. Bernadini, C., Felicetti, F., Meneghetti-Vitale, Penso, G., Overzoli, R., et al., Laboratori Nazionali di Frascati Report No. LNF-68/46 (unpublished, 1968).
170. Shyn, T. W., Williams, W. L., Robiscoe, R. T., Rebane, T., Phys. Rev. Letters 22, 1273 (1969).
171. Vorburger, T. V., Cosens, B. L., Phys. Rev. Letters 23, 1273 (1969).
172. Lipworth, E. and Novick, R., Phys. Rev. 108, 1434 (1957).
173. Narasimham, M. A., Ph.D. Thesis, University of Colorado, 1969 (unpublished).
174. Mader, D. and Leventhal, M., International Conf. on Atomic Physics, New York University (1968).
175. Hatfield, L. L. and Hughes, R. N., Phys. Rev. 156, 102 (1967).
176. Jacobs, R. R., Lea, K. R., Lamb, Jr., W. E., Bull. Am. Phys. Soc. 14, 525 (1969).
177. Fan, C. Y., Garcia-Munoz, M., Sellin, I. A., Phys. Rev. 161, 6 (1967).

FOOTNOTES

1. The survey of literature for this review was concluded in March 1970.
2. The most persuasive experimental evidence that the Josephson voltage-frequency relation $2eV = h\nu$ is exact has been provided by Clarke (37) who has compared, by a sensitive differential method, the voltage of the induced steps in Josephson junctions of different materials (Sn, Pb, In) exposed to the same rf field. It was found that the steps occurred at the same voltage, independent of junction material to within 1 part in 10^8 . Since the Josephson relation is based on general quantum mechanical arguments [see Feynman (38) for a clear physical derivation], and since the results are independent of macroscopic parameters it does not seem imprudent to trust the new order of magnitude of precision it gives to e/h over previous determinations. It has been, however, recently predicted (39) that vacuum polarization effects proportional to the electron density in the superconductor will become important at a precision of $1:10^{10}$.
3. A hopefully temporary exception to this is the muon moment or mass which enters the muonium hfs comparison. This is discussed later in this section.
4. Extensive theoretical work has been applied toward determining the asymptotic $q^2 \rightarrow \infty$ behavior of the form factors. For a review see Appelquist and Primack (48).

5. Hadronic corrections to positronium and muonium s-levels occur in order $\alpha(Z\alpha)^4 m_e^2/m_\pi^2$ through vacuum polarization. Weak corrections similar to Δa_μ (weak) are nominally the size of α^3/π^3 radiative correction.
6. When the Dirac theory is used, the states $|m\rangle$ include the "Z-graph" contributions (2 electrons plus a positron in the binding potential). These enter with opposite sign (because of the Pauli principle) to the one electron contributions and reduce the apparent linear divergence in 3.22 to a logarithmic divergence. [See V. S. Weiskopf in ref. (1).]
7. The relationship of 3.27 to the non-covariant expression 3.22 may be found in Erickson's thesis (Univ. of Minn., 1962, unpub.).
8. Only the $q_0 = 0$ part of this term is included in the Breit equation, which though non-covariant, does incorporate the correct reduced mass corrections to the fine structure spectrum.
9. The difference of $\nu_{\text{hfs}}(n=1)$ and $8 \nu_{\text{hfs}}(n=2)$ is independent of δ_N and is in good agreement with experiment (123,138,139).
10. In the double resonance method, two transitions between the Rabi-levels are measured at the same magnetic field, yielding both ν_{hfs} and the muon moment free of chemical shifts (V. Telegdi, private communication).

TABLE I

Recent High Energy Tests of QED

<u>Experiment</u>	<u>References</u>	<u>Parametrization</u>	<u>95% Confidence Limit</u>
$e^- + e^- \rightarrow e^- + e^-$ $\sqrt{s} = m_{e^+e^-} \sim 1110 \text{ MeV}/c^2$	Barber et al. (3) (Stanford-Princeton, 1968)	$F(q^2) = (1 - q^2/K^2)^{-1}$ $F(q^2) = (1 + q^2/K^2)^{-1}$	$K > 2.4 \text{ GeV}/c^2$ $K > 4.0 \text{ GeV}/c^2$
$e^+ + e^- \rightarrow e^+ + e^-$ $\sqrt{s} = m_{e^+e^-} \sim 1020 \text{ MeV}/c^2$	Augustin et al. (24) (Orsay, 1969)	$F(q^2) = (1 + q^2/K^2)^{-1}$	$K > 2.6 \text{ GeV}$
$\gamma + C \rightarrow C + e^+ + e^-$ $m_{e^+e^-} \leq 900 \text{ MeV}/c^2$	Alvensleben et al. (19) (DESY-MIT, 1968)	$\frac{\sigma_{\text{exp}}}{\sigma_{\text{Th}}} = 1 + m^4/\Lambda^4$	$\Lambda > 1.4 \text{ GeV}/c^2$
$\gamma + C \rightarrow C + e^+ + e^-$ $m_{e^+e^-} \leq 444 \text{ MeV}/c^2$	Tenenbaum et al. (10) (Harvard, 1969)	$\frac{\sigma_{\text{exp}}}{\sigma_{\text{Th}}} = 1 + m^4/\Lambda^4$	$\Lambda > 0.8 \text{ GeV}/c^2$
$\gamma + p \rightarrow p + e^+ + e^-$ $m_{e^+e^-} \leq 490 \text{ MeV}/c^2$	Biggs et al. (12) (Daresbury, 1969)	$\frac{\sigma_{\text{exp}}}{\sigma_{\text{Th}}} = 1 + m^4/\Lambda^4$	$\Lambda > 0.7 \text{ GeV}/c^2$

[See also Cohen et al., MIT, (163); Eisenhandler et al., Cornell, (164)]

(Table I con't.)

<u>Experiment</u>	<u>References</u>	<u>Parametrization</u>	<u>95% Confidence Limit</u>
$\gamma + C \rightarrow C + \mu^+ + \mu^-$ $m_{\mu^+\mu^-} \leq 1225 \text{ MeV}/c^2$ [See also dePagter et al., Northeastern (165); Quinn et al., Stanford (166)]	Hayes et al. (22) (Cornell, 1969)	$\frac{\sigma_{\text{exp}}}{\sigma_{\text{Th}}} = 1 - m^4/\Lambda^4$	$\Lambda > 1.5 \text{ GeV}/c^2$
$e^- + C \rightarrow e^- + C + \gamma$ $m_{e\gamma} \leq 1030 \text{ MeV}/c^2$	Siemann et al. (167) (Cornell, 1969)	$\frac{\sigma_{\text{exp}}}{\sigma_{\text{Th}}} = 1 + m^4/\Lambda^4$	$\Lambda > 1.5 \text{ GeV}/c^2$
$\mu + C \rightarrow \mu + C + \gamma$ $m_{\mu\gamma} \leq 650 \text{ MeV}/c^2$ [See also Bernardini et al., Frascati (169)]	Liberman et al. (168) (Harvard-Case-McGill)	$\frac{\sigma_{\text{exp}}}{\sigma_{\text{Th}}} = 1 + m^4/\Lambda^4$	$\Lambda > 0.7 \text{ GeV}/c^2$

TABLE II (From ref. 98)

VARIOUS CONTRIBUTIONS TO THE LAMB SHIFT IN H (n = 2)

DESCRIPTION	ORDER	MAGNITUDE (MHz)
2 nd ORDER — SELF-ENERGY	$\alpha(Z\alpha)^4 m \{ \log Z\alpha, 1 \}$	1079.32 ± 0.02
2 nd ORDER — VAC. POL.	$\alpha(Z\alpha)^4 m$	- 27.13
2 nd ORDER — REMAINDER	$\alpha(Z\alpha)^5 m$	7.14
	$\alpha(Z\alpha)^6 m \{ \log^2 Z\alpha, \log Z\alpha, 1 \}$	- 0.38 \pm 0.04
4 th ORDER — SELF-ENERGY	$\alpha^2 (Z\alpha)^4 m \begin{cases} F_1'(0) \\ F_2(0) \end{cases}$	0.45 ± 0.07 - 0.10
	$\alpha^2 (Z\alpha)^5 m$	± 0.02
4 th ORDER — VAC. POL.	$\alpha^2 (Z\alpha)^4 m$	- 0.24
REDUCED MASS CORRECTIONS	$\alpha(Z\alpha)^4 \frac{m}{M} m \{ \log Z\alpha, 1 \}$	- 1.64
RECOIL	$(Z\alpha)^5 \frac{m}{M} m \{ \log Z\alpha, 1 \}$	0.36 ± 0.01
PROTON SIZE	$(Z\alpha)^4 (mR_N)^2 m$	<u>0.13</u>

$$\alpha^{-1} = 137.03608(26)$$

$$\begin{aligned} \mathcal{L} &= \Delta E(2S_{\frac{1}{2}} - 2P_{\frac{1}{2}}) = 1057.91 \pm 0.16 \text{ (L. E.)} \\ &\Delta E(2P_{\frac{3}{2}} - 2S_{\frac{1}{2}}) = 9911.12 \pm 0.22 \text{ (L. E.)} \\ &\Delta E(2P_{\frac{3}{2}} - 2P_{\frac{1}{2}}) = 10969.03 \pm 0.12 \text{ (L. E.)} \end{aligned}$$

TABLE III(a)

THE LAMB SHIFT IN HYDROGENIC ATOMS (in MHz)

<u>Reference</u>	<u>$\mathcal{L}_{\text{exp}} (\pm 1\sigma)$</u>	<u>(Old) Theory (\pm L. E.)</u>	<u>(Old) Exp-Th ($\pm 1\sigma$)</u>	<u>Revised Theory (\pm L. E.)</u>	<u>Revised Exp-Th ($\pm 1\sigma$)</u>
H (n = 2)		1057.56 \pm 0.09		1057.91 \pm 0.16	
Triebwasser, Dayhoff, Lamb (109)	1057.77 \pm 0.06		0.21 \pm 0.07		- 0.14 \pm 0.08
Robiscoe (Revised, 113)	1057.90 \pm 0.06		0.34 \pm 0.07		- 0.01 \pm 0.08
Kaufman, Lea, Leventhal, Lamb (115) [($\Delta E - \mathcal{L}$) _{exp} = 9911.38 \pm 0.03]	(1057.65 \pm 0.05)		0.09 \pm 0.06		- 0.26 \pm 0.07
Shyn, Williams, Robiscoe, Rebane (170) [($\Delta E - \mathcal{L}$) _{exp} = 9911.25 \pm 0.06]	(1057.78 \pm 0.07)		0.22 \pm 0.08		- 0.13 \pm 0.09
Cosens and Vorburger (171) [($\Delta E - \mathcal{L}$) _{exp} = 9911.17 \pm 0.04]	(1057.86 \pm 0.06)		0.30 \pm 0.07		- 0.05 \pm 0.08
D (n = 2)		1058.82 \pm 0.15		1059.17 \pm 0.22	
Triebwasser, Dayhoff, Lamb (109)	1059.00 \pm 0.06		0.18 \pm 0.08		- 0.17 \pm 0.09
Cosens (114, 171)	1059.28 \pm 0.06		0.46 \pm 0.08		+ 0.11 \pm 0.09

TABLE III(b)

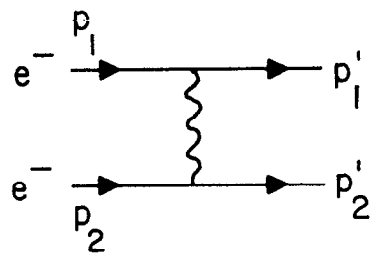
LAMB SHIFT IN OTHER HYDROGENIC ATOMS

<u>Reference</u>	<u>$\mathcal{L}_{\text{exp}} (\pm 1\sigma)$</u>	<u>Old Theory (\pm L.E.)</u>	<u>Old Exp-Th ($\pm 1\sigma$)</u>	<u>Revised Theory (\pm L.E.)</u>	<u>Revised Exp-Th ($\pm 1\sigma$)</u>
He ⁺ (n = 2)		14038.9 \pm 4.1		14044.5 \pm 5.2	
Lipworth, Novick (172)	14040.2 \pm 1.8		1.3 \pm 2.2		- 4.3 \pm 2.5
Narasimham (173)	14045.4 \pm 1.2		6.5 \pm 1.8		1.0 \pm 2.1
He ⁺ (n = 3)		4182.7 \pm 1.2		4184.4 \pm 1.5	
Mader, Leventhal (174, 34)	4182.4 \pm 1.0		-0.3 \pm 1.1		- 2.0 \pm 1.1
Mader, Leventhal (174)	(4184.0 \pm 0.6)		1.3 \pm 0.7		- 0.4 \pm 0.8
[$\Delta E - \mathcal{L} = 47843.8 \pm 0.5$]					
He ⁺ (n = 4)		1768.3 \pm 0.5		1769.0 \pm 0.6	
Hatfield, Hughes (175)	1776.0 \pm 7.5		-2.3 \pm 7.5		- 3.0 \pm 7.5
Jacobs, Lea, Lamb (176, 34)	1768.0 \pm 5.0		-0.3 \pm 5.0		- 1.0 \pm 5.0
Jacobs, Lea, Lamb (176)	(1769.4 \pm 1.2)		+1.1 \pm 1.3		0.4 \pm 1.3
[$\Delta E - \mathcal{L} = 20179.7 \pm 1.2$]					
Li ⁺⁺ (n = 2)		62743.0 \pm 45.0		62771.0 \pm 50.0	
Fan, Garcia-Munoz, Sellin (177)	63031.0 \pm 327.0		288.0 \pm 333.0		260.0 \pm 333.0

Figure Captions

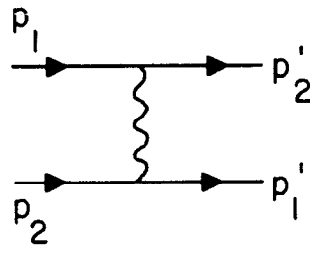
- Fig. 1. Born diagrams for electron-electron elastic scattering.
- Fig. 2. Born diagrams for electron-positron elastic scattering.
- Fig. 3. Electron-positron annihilation into muon pairs, including vacuum polarization modifications.
- Fig. 4. Born diagrams for electron-positron annihilation into two photons.
- Fig. 5. (a) Bethe-Heitler diagrams for pair production on a nucleus. (b) Virtual Compton amplitude for pair production. (c) Bethe-Heitler diagrams for bremsstrahlung on a nucleus. (d) Virtual Compton amplitude for bremsstrahlung. The exchanged photon attaches at each open circle in diagrams (a) and (c).
- Fig. 6. (a) Born diagrams for trident production on a nucleus. Four Feynman diagrams are generated by attaching the nuclear photon to each open circle. In the case of identical particles, four additional exchange diagrams are to be included. (b) Virtual Compton amplitude for trident production.
- Fig. 7. Composite picture of high energy measurements, with 95% confidence (in GeV) on possible modifications of the photon and lepton space-like and time-like propagators. See Table I and text.

- Fig. 8. Two particle intermediate state contribution to the lepton vertex using sidewise-dispersion relations. In the threshold region, the required Compton amplitude is given by the low energy theorem.
- Fig. 9. Distribution of decay-electron events as a function of time. Lower curve shows rotation frequency of muon. The upper curves show the $g-2$ precession. [From Bailey et al., ref. 59.]
- Fig. 10. Photon-photon scattering contribution to the sixth order magnetic moment of the muon calculated in ref. 57. Five other Feynman diagrams are obtained from crossing the photon legs. A similar set of diagrams contributes to the electron moment.
- Fig. 11. Hadronic vacuum polarization correction to the muon magnetic moment.
- Fig. 12. $n = 1$ and $n = 2$ levels of the hydrogen atom.
- Fig. 13. Typical irreducible kernels of the Bethe-Salpeter equation which are included in the theoretical analysis of the hydrogen spectrum.



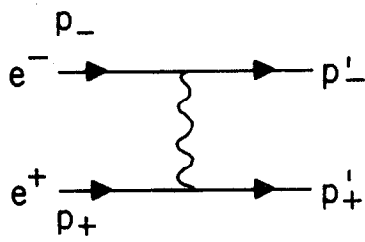
(a)

+



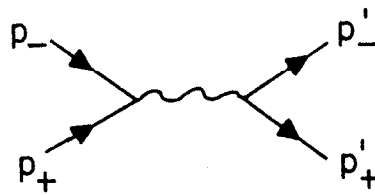
(b)

Fig. 1



(a)

+



(b)

Fig. 2

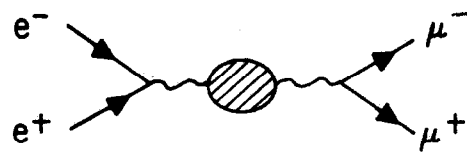


Fig. 3

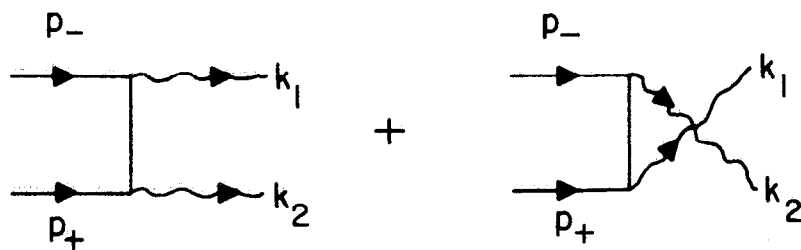


Fig. 4

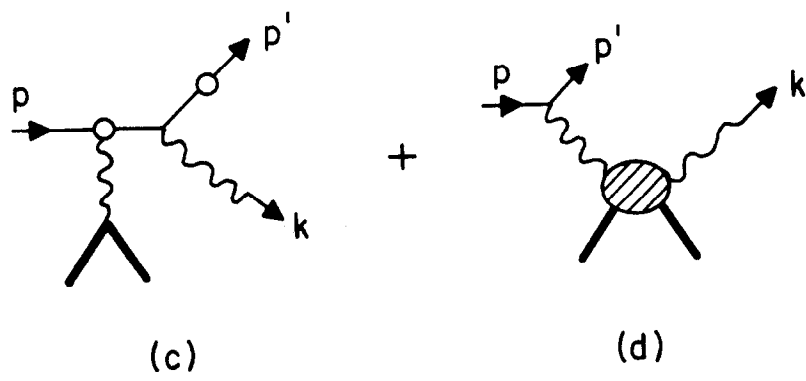
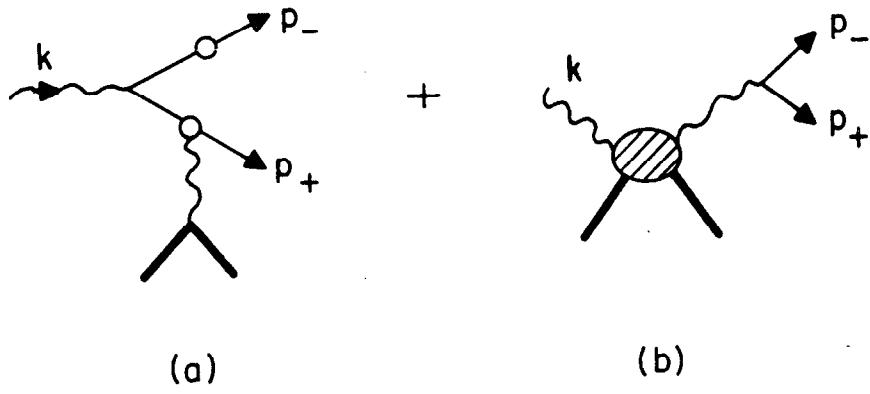


Fig. 5

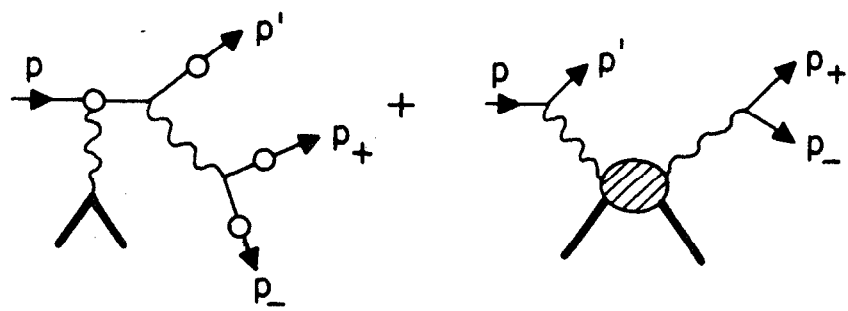


Fig. 6

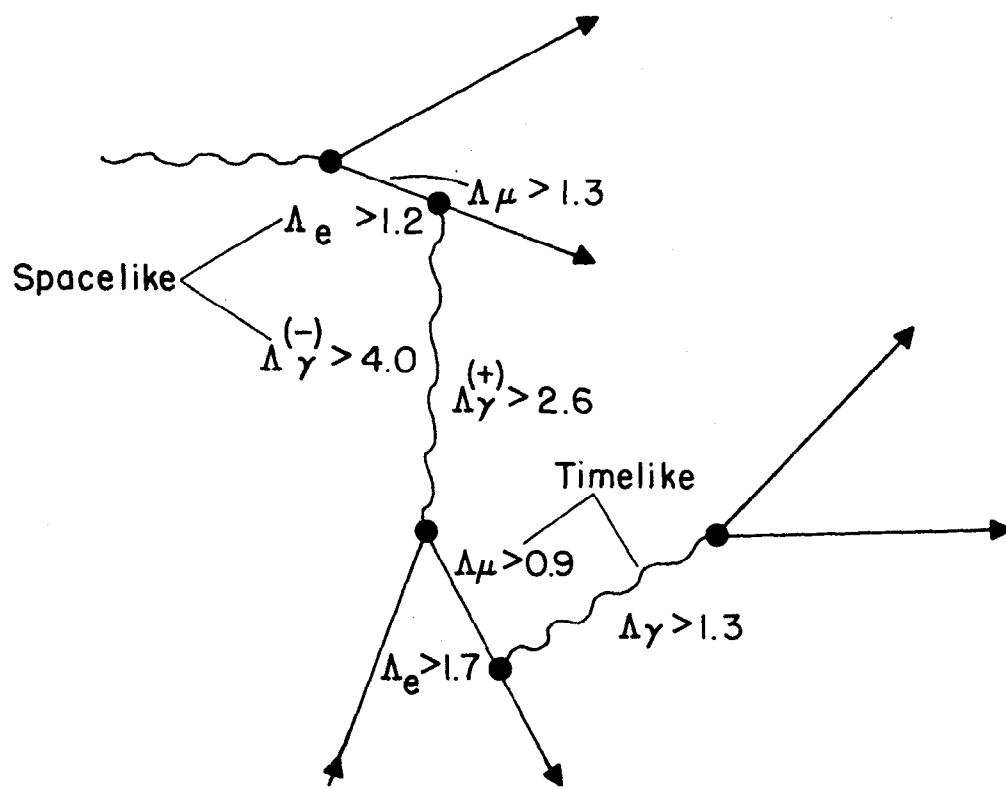


Fig. 7.

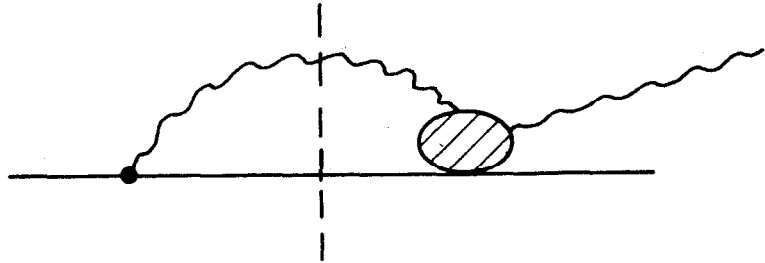


Fig. 8

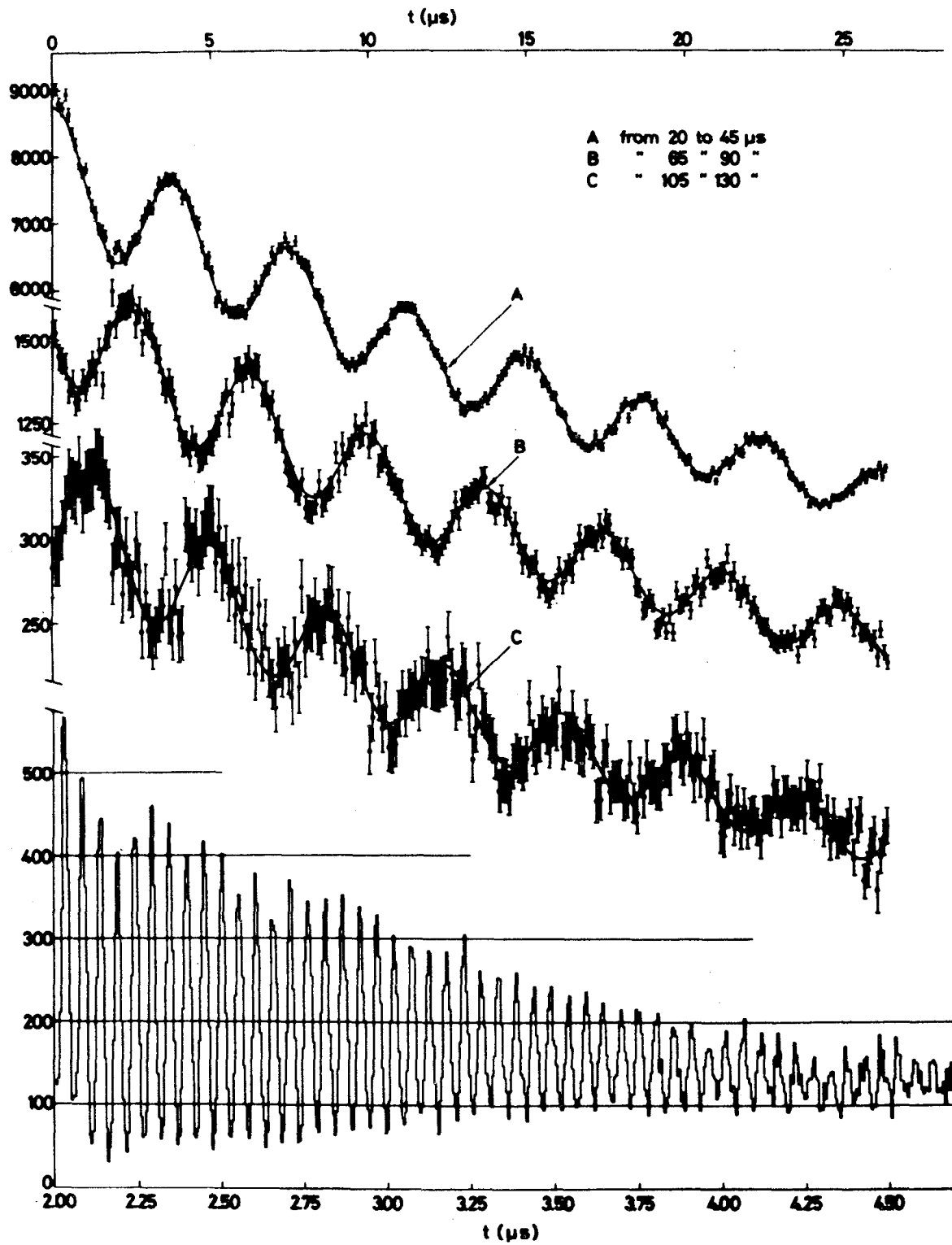


Fig. 9

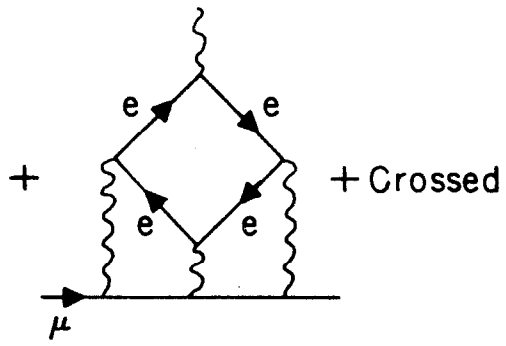


Fig. 10

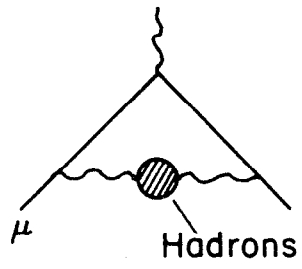
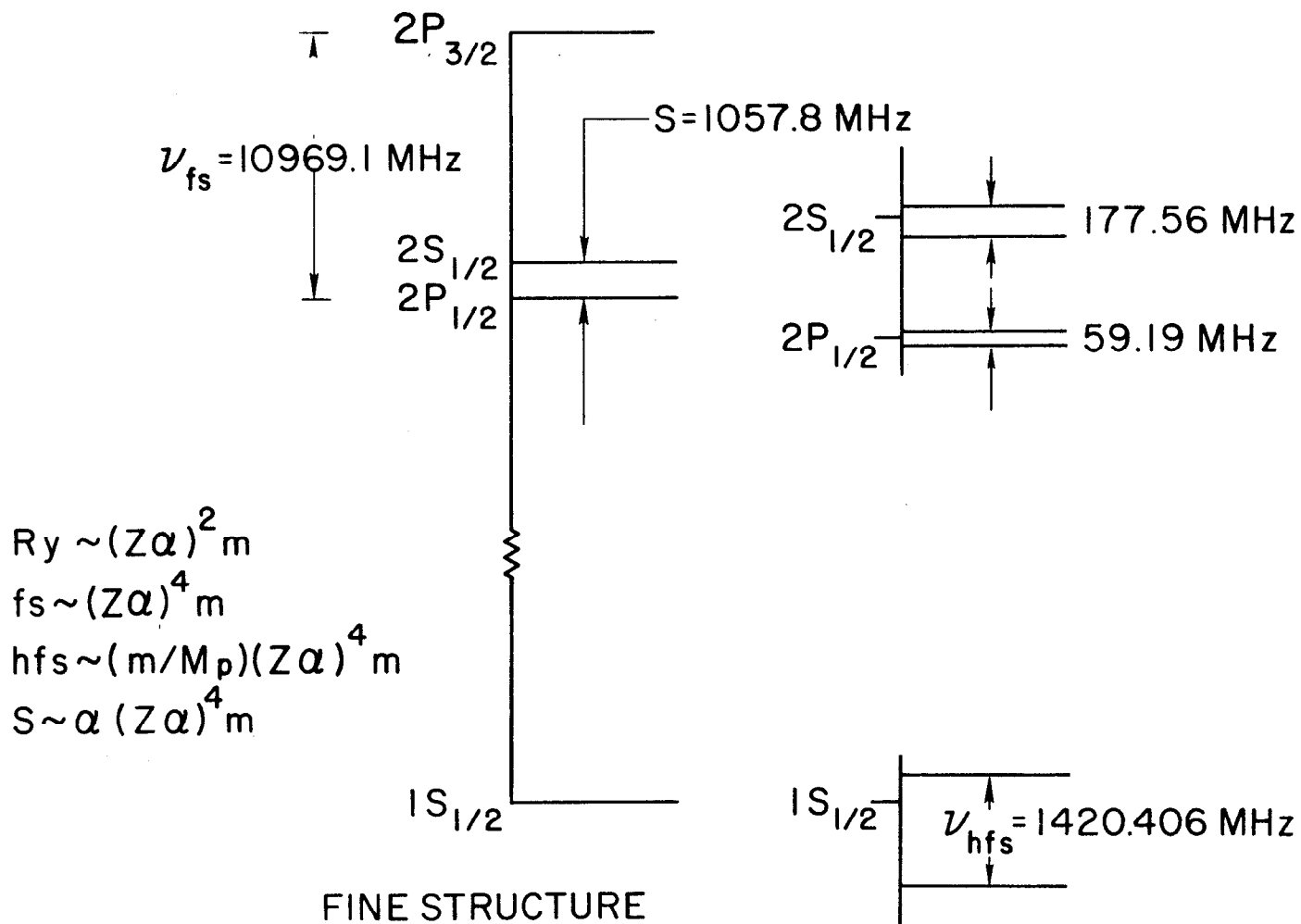


Fig. 11

THE HYDROGEN ATOM



FINE STRUCTURE

HYPERFINE STRUCTURE

Fig. 12

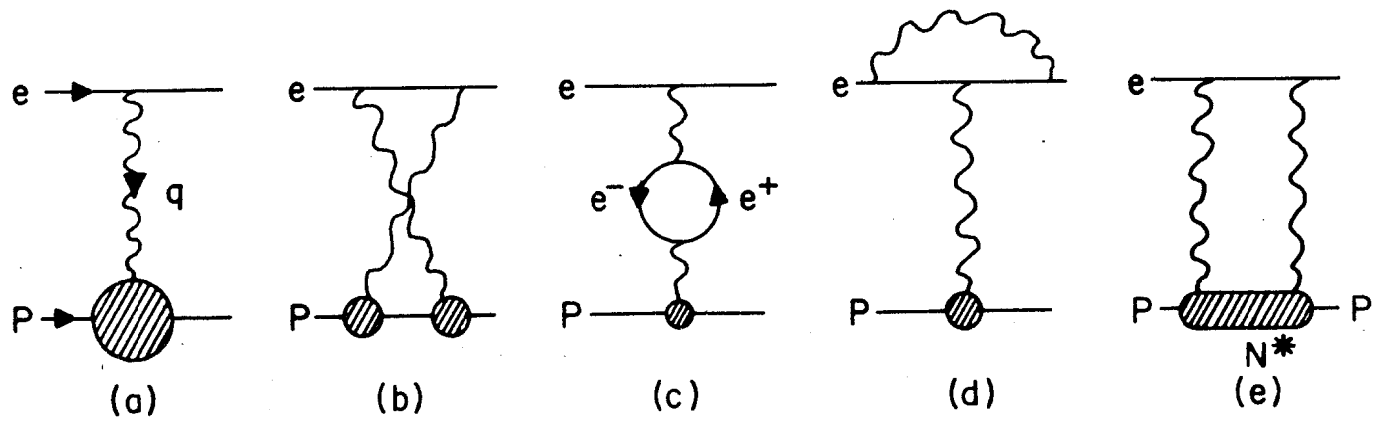


Fig. 13